ASM Handbook, Volume 1: Properties and Selection: Irons, Steels, and High-Performance Alloys
ASM Handbook Committee, p 673-688

Fatigue Resistance of Steels

Bruce Boardman, Deere and Company, Technical Center

FATIGUE is the progressive, localized, and permanent structural change that occurs in a material subjected to repeated or fluctuating strains at nominal stresses that have maximum values less than (and often much less than) the tensile strength of the material. Fatigue may culminate into cracks and cause fracture after a sufficient number of fluctuations. The process of fatigue consists of three stages:

- Initial fatigue damage leading to crack initiation
- Crack propagation to some critical size (a size at which the remaining uncracked cross section of the part becomes too weak to carry the imposed loads)
- Final, sudden fracture of the remaining cross section

Fatigue damage is caused by the simultaneous action of cyclic stress, tensile stress, and plastic strain. If any one of these three is not present, a fatigue crack will not initiate and propagate. The plastic strain resulting from cyclic stress initiates the crack; the tensile stress promotes crack growth (propagation). Careful measurement of strain shows that microscopic plastic strains can be present at low levels of stress where the strain might otherwise appear to be totally elastic. Although compressive stresses will not cause fatigue, compressive loads may result in local tensile stresses.

In the early literature, fatigue fractures were often attributed to crystallization because of their crystalline appearance. Because metals are crystalline solids, the use of the term crystallization in connection with fatigue is incorrect and should be avoided.

Fatigue Resistance

Variations in mechanical properties, composition, microstructure, and macrostructure, along with their subsequent effects on fatigue life, have been studied extensively to aid in the appropriate selection of steel to meet specific end-use requirements. Studies have shown that the fatigue strength of steels is usually proportional to hardness and tensile strength; this generalization is not true, however, for high tensile strength values where toughness and critical flaw size may govern ultimate load carrying ability. Processing, fabrication, heat treatment, surface treatments, finishing, and service environments significantly influence the ultimate behavior of a metal subjected to cyclic stressing.

Predicting the fatigue life of a metal part is complicated because materials are sensitive to small changes in loading conditions and stress concentrations and to other factors. The resistance of a metal structural member to fatigue is also affected by manufacturing procedures such as cold forming, welding, brazing, and plating and by surface conditions such as surface roughness and residual stresses. Fatigue tests performed on small specimens are not sufficient for precisely establishing the fatigue life of a part. These tests are useful for rating the relative resistance of a material and the baseline properties of the material to cyclic stressing. The baseline properties must be combined with the load history of the part in a design analysis before a component life prediction can be made.

In addition to material properties and loads, the design analysis must take into consideration the type of applied loading (uniaxial, bending, or torsional), loading pattern (either periodic loading at a constant or variable amplitude or random loading), magnitude of peak stresses, overall size of the part, fabrication method, surface roughness, presence of fretting or corroded surface, operating temperature and environment, and occurrence of service-induced imperfections.

Traditionally, fatigue life has been expressed as the total number of stress cycles required for a fatigue crack to initiate and grow large enough to produce catastrophic failure, that is, separation into two pieces. In this article, fatigue data are expressed in terms of total life. For the small samples that are used in the laboratory to determine fatigue properties, this is generally the case; but, for real components, crack initiation may be as little as a few percent or the majority of the total component life.

Fatigue data can also be expressed in terms of crack growth rate. In the past, it was commonly assumed that total fatigue life consisted mainly of crack initiation (stage I of fatigue crack development) and that the time required for a minute fatigue crack to grow and produce failure was a minor portion of the total life. However, as better methods of crack detection became available, it was discovered that cracks often develop early in the fatigue life of the material (after as little as 10% of total lifetime) and grow continuously until catastrophic failure occurs. This discovery has led to the use of crack growth rate, critical crack size, and fracture mechanics for the prediction of total life in some applications. Hertzberg's text (Ref 1) is a useful primer for the use of fracture mechanics methods.

Prevention of Fatigue Failure

A thorough understanding of the factors that can cause a component to fail is essential before designing a part. Reference 2 provides numerous examples of these factors that cause fracture (including fatigue) and includes high-quality optical and electron micrographs to help explain factors.

The incidence of fatigue failure can be considerably reduced by careful attention to design details and manufacturing processes. As long as the metal is sound and free from major flaws, a change in material composition is not as effective for achieving satisfactory fatigue life as is care taken in design, fabrication, and maintenance during service. The most effective and economical method of improving fatigue performance is improvement in design to:

- Eliminate or reduce stress raisers by streamlining the part
- Avoid sharp surface tears resulting from punching, stamping, shearing, and so on
- Prevent the development of surface discontinuities or decarburizing during processing or heat treatment
- Reduce or eliminate tensile residual stresses caused by manufacturing, heat treating, and welding
- Improve the details of fabrication and fastening procedures

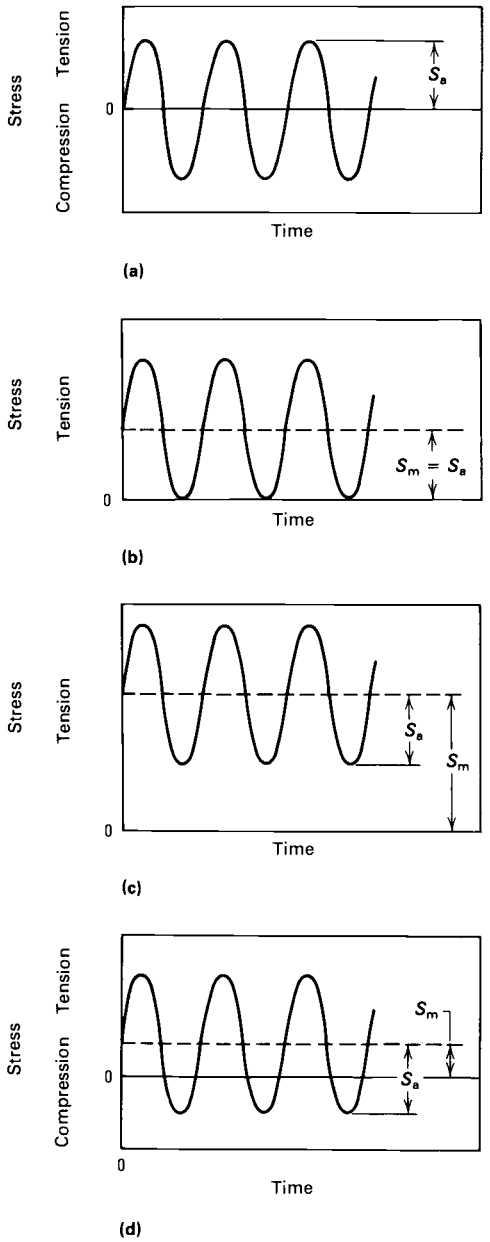

Fig. 1 Types of fatigue test stress. (a) Alternating stress in which $S_m = 0$ and $R = -1$. (b) Pulsating tensile stress in which $S_m = S_a$, the minimum stress is zero, and $R = 0$. (c) Fluctuating tensile stress in which both the minimum and maximum stresses are tensile stresses and $R = \frac{1}{3}$. (d) Fluctuating tensile-to-compressive stress in which the minimum stress is a compressive stress, the maximum stress is a tensile stress, and $R = -\frac{1}{3}$

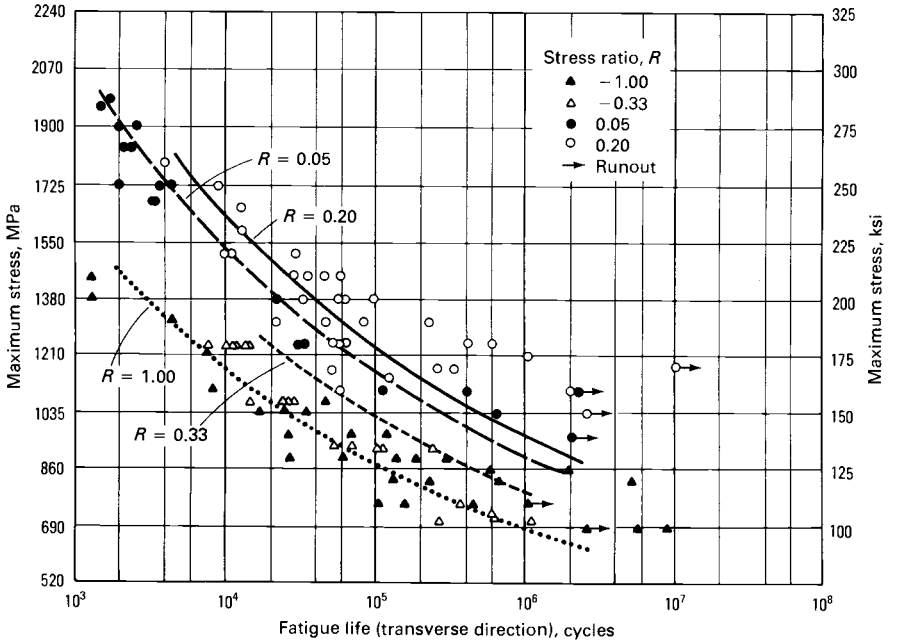

Fig. 2 Best-fit *S-N* curves for unnotched 300M alloy forging with an ultimate tensile strength of 1930 MPa (280 ksi). Stresses are based on net section. Testing was performed in the transverse direction with a theoretical stress concentration factor, K_t, of 1.0. Source: Ref 4

Control of or protection against corrosion, erosion, chemical attack, or service-induced nicks and other gouges is an important part of proper maintenance of fatigue life during active service life. Reference 3 contains numerous papers pertaining to these subjects.

Symbols and Definitions

In most laboratory fatigue testing, the specimen is loaded so that stress is cycled either between a maximum and a minimum tensile stress or between a maximum tensile stress and a specified level of compressive stress. The latter of the two, considered a negative tensile stress, is given an algebraic minus sign and called the minimum stress.

Applied Stresses. The mean stress, S_m, is the algebraic average of the maximum stress and the minimum stress in one cycle:

$$S_m = \frac{(S_{max} + S_{min})}{2} \quad \text{(Eq 1)}$$

The range of stress, S_r, is the algebraic difference between the maximum stress and the minimum stress in one cycle:

$$S_r = S_{max} - S_{min} \quad \text{(Eq 2)}$$

The stress amplitude, S_a, is one-half the range of stress:

$$S_a = \frac{S_r}{2} = \frac{(S_{max} - S_{min})}{2} \quad \text{(Eq 3)}$$

During a fatigue test, the stress cycle is usually maintained constant so that the applied stress conditions can be written $S_m \pm S_a$, where S_m is the static or mean stress and S_a is the alternating stress equal to one-half the stress range. The positive sign is used to denote a tensile stress, and the negative sign denotes a compressive stress. Some of the possible combinations of S_m and S_a are shown in Fig. 1. When $S_m = 0$ (Fig. 1a), the maximum tensile stress is equal to the maximum compressive stress; this is called an alternating stress, or a completely reversed stress. When $S_m = S_a$ (Fig. 1b), the minimum stress of the cycle is zero; this is called a pulsating, or repeated, tensile stress. Any other combination is known as an alternating stress, which may be an alternating tensile stress (Fig. 1c), an alternating compressive stress, or a stress that alternates between a tensile and a compressive value (Fig. 1d).

Nominal axial stresses can be calculated on the net section of a part (S = force per unit area) without consideration of variations in stress conditions caused by holes, grooves, fillets, and so on. Nominal stresses are frequently used in these calculations, although a closer estimate of actual stresses through the use of a stress concentration factor might be preferred.

Stress ratio is the algebraic ratio of two specified stress values in a stress cycle. Two commonly used stress ratios are A, the ratio of the alternating stress amplitude to the mean stress ($A = S_a/S_m$) and R, the ratio of the minimum stress to the maximum stress ($R = S_{min}/S_{max}$). The five conditions that R can take range from +1 to −1:

- Stresses are fully reversed: $R = -1$
- Stresses are partially reversed: R is between −1 and zero
- Stress is cycled between a maximum stress and no load: The stress ratio R becomes zero
- Stress is cycled between two tensile stresses: The stress ratio R becomes a positive number less than 1
- An R stress ratio of 1 indicates no variation in stress, and the test becomes a sustained-load creep test rather than a fatigue test

***S-N* Curves.** The results of fatigue tests are usually plotted as the maximum stress or

stress amplitude versus the number of cycles, N, to fracture, using a logarithmic scale for the number of cycles. Stress may be plotted on either a linear or a logarithmic scale. The resulting curve of data points is called an S-N curve. A family of S-N curves for a material tested at various stress ratios is shown in Fig. 2. It should be noted that the fully reversed condition, $R = -1$, is the most severe, with the least fatigue life. For carbon and low-alloy steels, S-N curves (plotted as linear stress versus log life) typically have a fairly straight slanting portion with a negative slope at low cycles, which changes with a sharp transition into a straight, horizontal line at higher cycles.

An S-N curve usually represents the median, or B_{50}, life, which represents the number of cycles when half the specimens fail at a given stress level. The scatter of fatigue lives covers a very wide range and can occur for many reasons other than material variability.

A constant-lifetime diagram (Fig. 3) is a summary graph prepared from a group of S-N curves of a material; each S-N curve is obtained at a different stress ratio. The diagram shows the relationship between the alternating stress amplitude and the mean stress and the relationship between maximum stress and minimum stress of the stress cycle for various constant lifetimes. Although this technique has received considerable use, it is now out of date. Earlier editions of the *Military Standardization Handbook* (Ref 5) used constant lifetime diagrams extensively, but more recent editions (Ref 4) no longer include them.

Fatigue limit (or endurance limit) is the value of the stress below which a material can presumably endure an infinite number of stress cycles, that is, the stress at which the S-N diagram becomes and appears to remain horizontal. The existence of a fatigue limit is typical for carbon and low-alloy steels. For many variable-amplitude loading conditions this is true; but for conditions involving periodic overstrains, as is typical for many actual components, large changes in the long-life fatigue resistance can occur (see the discussion in the section "Comparison of Fatigue Testing Techniques" in this article).

Fatigue strength, which should not be confused with fatigue limit, is the stress to which the material can be subjected for a specified number of cycles. The term fatigue strength is used for materials, such as most nonferrous metals, that do not exhibit well-defined fatigue limits. It is also used to describe the fatigue behavior of carbon and low-alloy steels at stresses greater than the fatigue limit.

Stress Concentration Factor. Concentrated stress in a metal is evidenced by surface discontinuities such as notches, holes, and scratches and by changes in microstructure

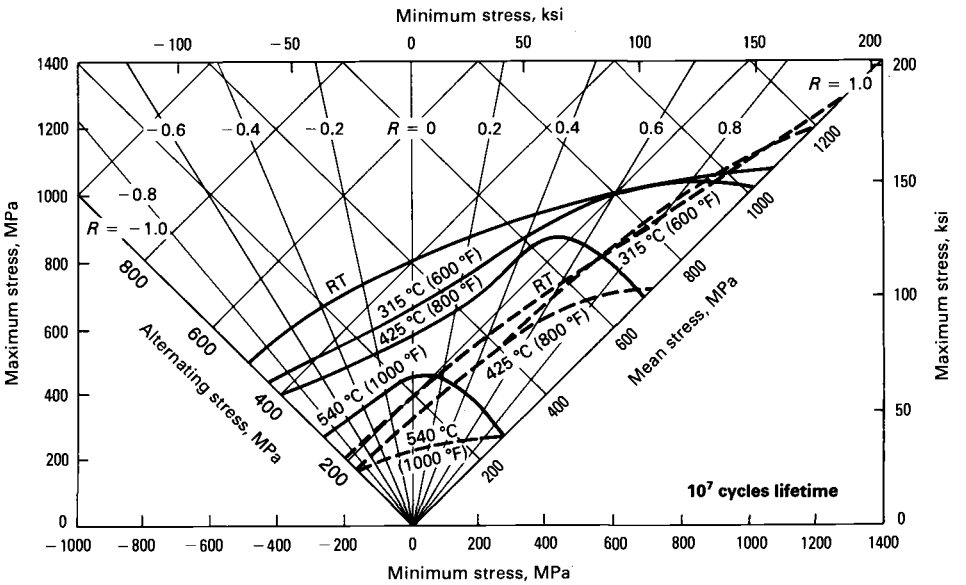

Fig. 3 Constant-lifetime fatigue diagram for AISI-SAE 4340 alloy steel bars, hardened and tempered to a tensile strength of 1035 MPa (150 ksi) and tested at various temperatures. Solid lines represent data obtained from unnotched specimens; dashed lines represent data from specimens having notches with $K_t = 3.3$. All lines represent lifetimes of ten million cycles. Source: Ref 5

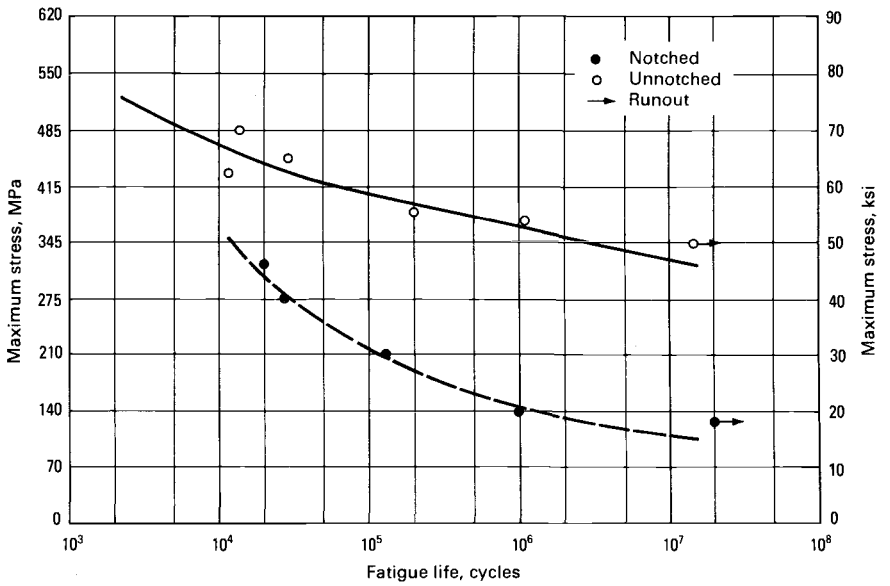

Fig. 4 Room temperature S-N curves for notched and unnotched AISI 4340 alloy steel with a tensile strength of 860 MPa (125 ksi). Stress ratio, R, equals −1.0. Source: Ref 4

such as inclusions and thermal heat affected zones. The theoretical stress concentration factor, K_t, is the ratio of the greatest elastically calculated stress in the region of the notch (or other stress concentrator) to the corresponding nominal stress. For the determination of K_t, the greatest stress in the region of the notch is calculated from the theory of elasticity or by finite-element analysis. Equivalent values may be derived experimentally. An experimental stress concentration factor is a ratio of stress in a notched specimen to the stress in a smooth (unnotched) specimen.

Fatigue notch factor, K_f, is the ratio of the fatigue strength of a smooth (unnotched) specimen to the fatigue strength of a notched specimen at the same number of cycles. The fatigue notch factor will vary with the life on the S-N curve and with the mean stress. At high stress levels and short cycles, the factor is usually less than at lower stress levels and longer cycles because of a reduction of the notch effect by plastic deformation.

Fatigue notch sensitivity, q, is determined by comparing the fatigue notch factor, K_f, and the theoretical stress concentration fac-

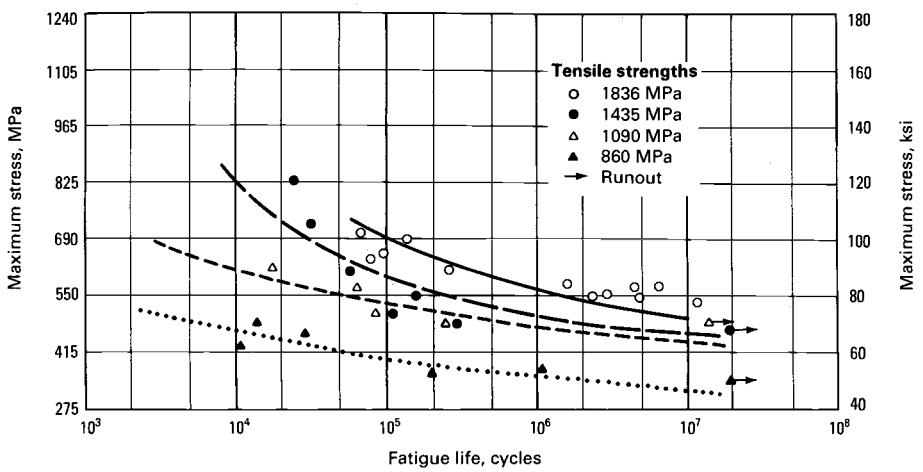

Fig. 5 Room temperature *S-N* curves for AISI 4340 alloy steel with various ultimate tensile strengths and with $R = -1.0$. Source: Ref 4

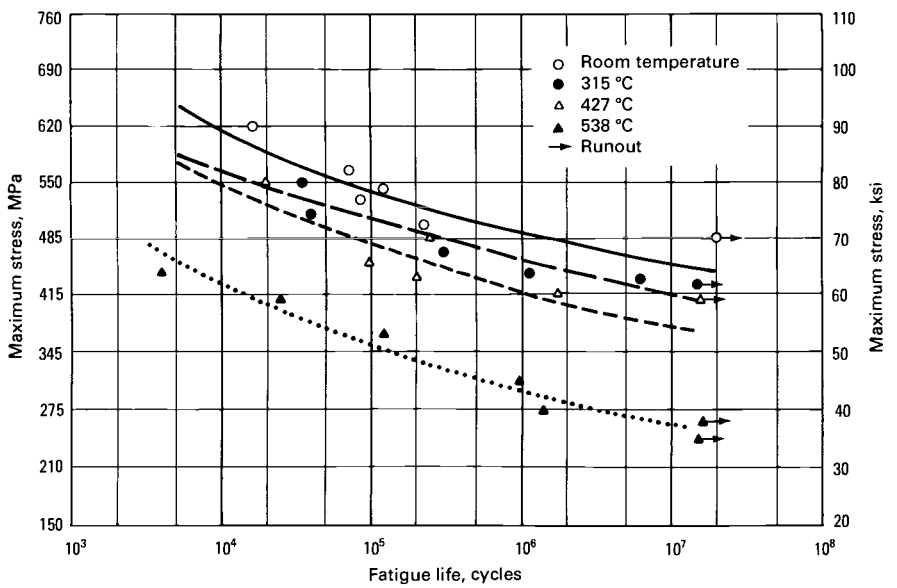

Fig. 6 *S-N* curves at various temperatures for AISI 4340 alloy steel with an ultimate tensile strength of 1090 MPa (158 ksi). Stress ratio, *R*, equals −1.0. Source: Ref 4

tor, K_t, for a specimen of a given size containing a stress concentrator of a given shape and size. A common definition of fatigue notch sensitivity is:

$$q = \frac{K_f - 1}{K_t - 1} \qquad \text{(Eq 4)}$$

in which q may vary between 0 (where $K_f = 1$, no effect) and 1 (where $K_f = K_t$, full effect). This value may be stated as a percentage. As the fatigue notch factor varies with the position on the *S-N* curve, so does notch sensitivity. Most metals tend to become more notch sensitive at low stresses and long cycles. If they do not, it may be that the fatigue strengths for the smooth (unnotched) specimens are lower than they could be because of surface imperfections. Most metals are not fully notch sensitive under high stresses and a low number of cycles. Under these conditions, the actual peak stress at the base of the notch is partly in the plastic strain condition. This results in the actual peak stress being lower than the theoretical peak elastic stress used in the calculation of the theoretical stress concentration factor.

Stress-Based Approach To Fatigue

The design of a machine element that will be subjected to cyclic loading can be approached by adjusting the configuration of the part so that the calculated stresses fall safely below the required line on an *S-N* plot. In a stress-based analysis, the material is assumed to deform in a nominally elastic manner, and local plastic strains are neglected. To the extent that these approximations are valid, the stress-based approach is useful. These assumptions imply that all the stresses will essentially be elastic.

The *S-N* plot shown in Fig. 4 presents data for AISI-SAE 4340 steel, heat treated to a tensile strength of 1035 MPa (150 ksi) in the notched and unnotched condition. Figure 5 shows the combinations of cyclic stresses that can be tolerated by the same steel when the specimens are heat treated to different tensile strengths ranging from 860 to 1790 MPa (125 to 260 ksi).

The effect of elevated temperature on the fatigue behavior of 4340 steel heat treated to 1035 MPa (150 ksi) is shown in Fig. 6. An increase in temperature reduces the fatigue strength of the steel and is most deleterious for those applications in which the stress ratio, R, lies between 0.4 and 1.0 (Fig. 3). A decrease in temperature may increase the fatigue limit of steel; however, parts with preexisting cracks may also show decreased total life as temperature is lowered, because of accompanying reductions in critical crack size and fracture toughness.

Figure 7 shows the effect of notches on the fatigue behavior of the ultrahigh-strength 300M steel. A K_t value of 2 is obtained in a specimen having a notch radius of about 1 mm (0.040 in.). For small parts, such a radius is often considered large enough to negate the stress concentration associated with any change in section. The significant effect of notches, even those with low stress concentration factors, on the fatigue behavior of this steel is apparent.

Data such as those presented in Fig. 3 to 7 may not be directly applicable to the design of structures because these graphs do not take into account the effect of the specific stress concentration associated with reentrant corners, notches, holes, joints, rough surfaces, and other similar conditions present in fabricated parts. The localized high stresses induced in fabricated parts by stress raisers are of much greater importance for cyclic loading than for static loading. Stress raisers reduce the fatigue life significantly below those predicted by the direct comparison of the smooth specimen fatigue strength with the nominal calculated stresses for the parts in question. Fabricated parts in simulated service have been found to fail at less than 50 000 repetitions of load, even though the nominal stress was far below that which could be repeated many millions of times on a smooth, machined specimen.

Correction Factors for Test Data. The available fatigue data normally are for a specific type of loading, specimen size, and surface roughness. For instance, the R.R. Moore rotating-beam fatigue test machine uses a 7.5 mm (0.3 in.) diam specimen that is free of any stress concentrations (because of specimen shape and a surface that has been polished to a mirror finish), and that is subjected to completely reversed bending stresses. For the fatigue

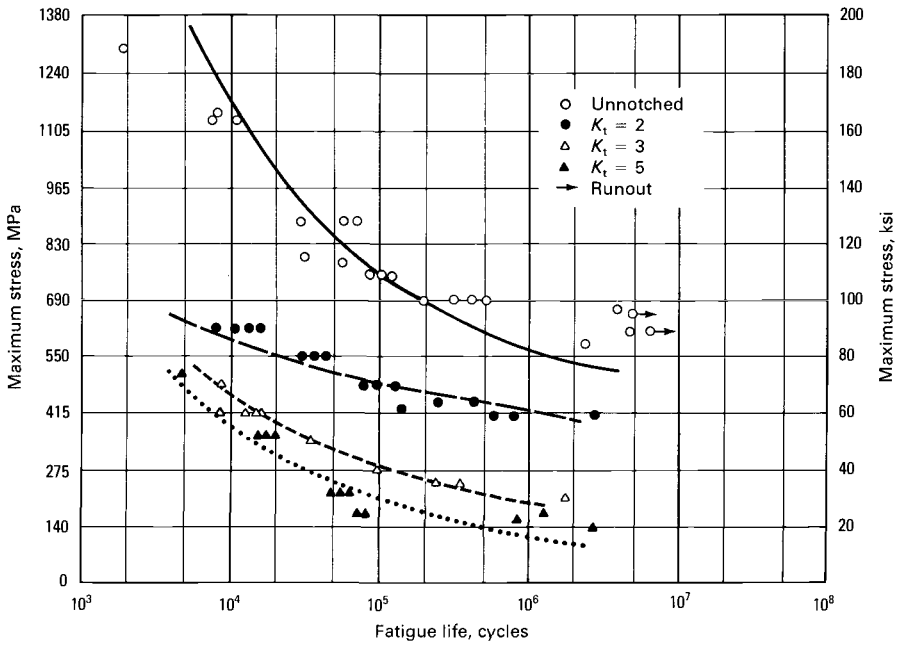

Fig. 7 Room-temperature *S-N* curves for a 300M steel with an ultimate tensile strength of 2000 MPa (290 ksi) having various notch severities. Stress ratio, *R*, equals 1.0. Source: Ref 4

limits used in design calculations, Juvinall (Ref 6) suggests the correction of fatigue life data by multiplying the fatigue limit from testing, N_i, by three factors that take into account the variation in the type of loading, part diameter, and surface roughness:

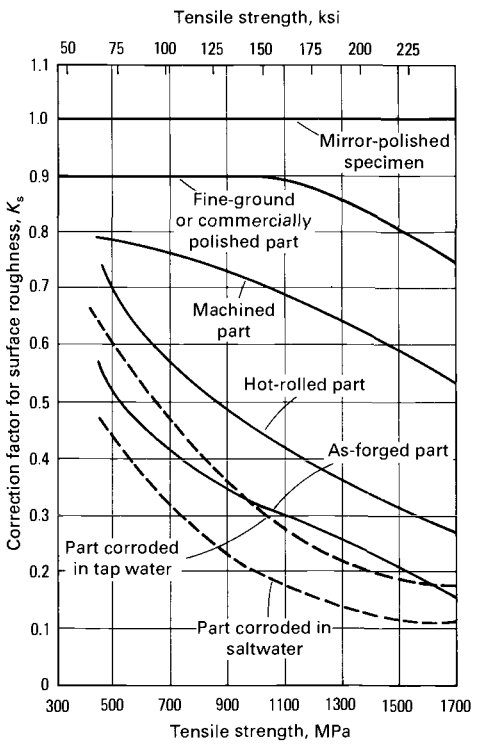

Fig. 8 Surface roughness correction factors for standard rotating-beam fatigue life testing of steel parts. See Table 1 for correction factors from part diameter and type of loading. Source: Ref 6

$$\textit{Design fatigue limit} = K_l \cdot K_d \cdot K_s \cdot N_i \qquad \text{(Eq 5)}$$

where K_l is the correction factor for the type of loading, K_d for the part diameter, and K_s for the surface roughness. Values of these factors are given in Table 1 and Fig. 8.

Strain-Based Approach To Fatigue

A strain-based approach to fatigue, developed for the analysis of low-cycle fatigue data, has proved to be useful for analyzing long-life fatigue data as well. The approach can take into account both elastic and plastic responses to applied loadings. The data are presented on a log-log plot similar in shape to an *S-N* curve; the value plotted on

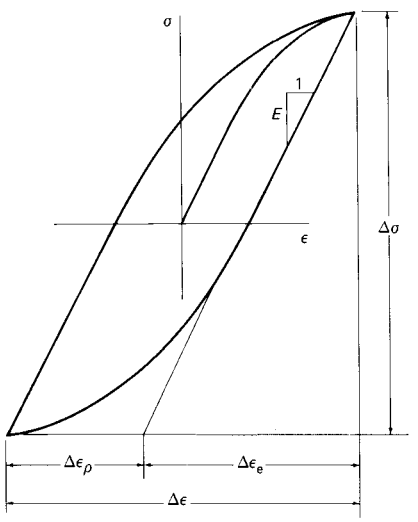

Fig. 9 Stress-strain hysteresis loop. Source: Ref 7

Table 1 Correction factors for surface roughness (K_s), type of loading (K_l), and part diameter (K_d), for fatigue life of steel parts

Factor	Value for loading in Bending	Torsion	Tension
K_l	1.0	0.58	0.9(a)
K_d			
where $d \leq 10$ mm (0.4 in.)	1.0	1.0	1.0
where 10 mm (0.4 in.) $< d \leq 50$ mm (2 in.)	0.9	0.9	1.0
K_s	See Fig. 8.		

(a) A lower value (0.06 to 0.85) may be used to take into account known or suspected undetermined bending because of load eccentricity. Source: Ref 6

the abscissa is the number of strain reversals (twice the number of cycles) to failure, and the ordinate is the strain amplitude (half the strain range).

During cyclic loading, the stress-strain relationship can usually be described by a loop, such as that shown in Fig. 9. For purely elastic loading, the loop becomes a straight line whose slope is the elastic modulus, *E*, of the material. The occurrence of a hysteresis loop is most common. The definitions of the plastic strain range, $\Delta\epsilon_p$, the elastic strain range, $\Delta\epsilon_e$, the total strain range, $\Delta\epsilon_t$, and the stress range, $\Delta\sigma$, are indicated in Fig. 9. A series of fatigue tests, each having a different total strain range, will generate a series of hysteresis loops. For each set of conditions, a characteristic number of strain reversals is necessary to cause failure.

As shown in Fig. 10, a plot on logarithmic coordinates of the plastic portion of the strain amplitude (half the plastic strain range) versus the fatigue life often yields a straight line, described by the equation:

$$\frac{\Delta\epsilon_p}{2} = \epsilon_f'(2N_f)^c \qquad \text{(Eq 6)}$$

where ϵ_f' is the fatigue ductility coefficient, *c* is the fatigue ductility exponent, and N_f is the number of cycles to failure.

Because the conditions under which elastic strains have the greatest impact on fatigue behavior are the long-life conditions where stress-based analysis of fatigue is appropriate, the effects of elastic strain on fatigue are charted by plotting stress amplitude (half the stress range) versus fatigue life on logarithmic coordinates. As shown in Fig. 11, the result is a straight line having the equation:

$$\frac{\Delta\sigma}{2} = \sigma_f'(2N_f)^b \qquad \text{(Eq 7)}$$

where σ_f' is the fatigue strength coefficient and *b* is the fatigue strength exponent.

The elastic strain range is obtained by dividing Eq 7 by *E*:

$$\frac{\Delta\epsilon_e}{2} = \frac{\sigma_f'}{E}(2N_f)^b \qquad \text{(Eq 8)}$$

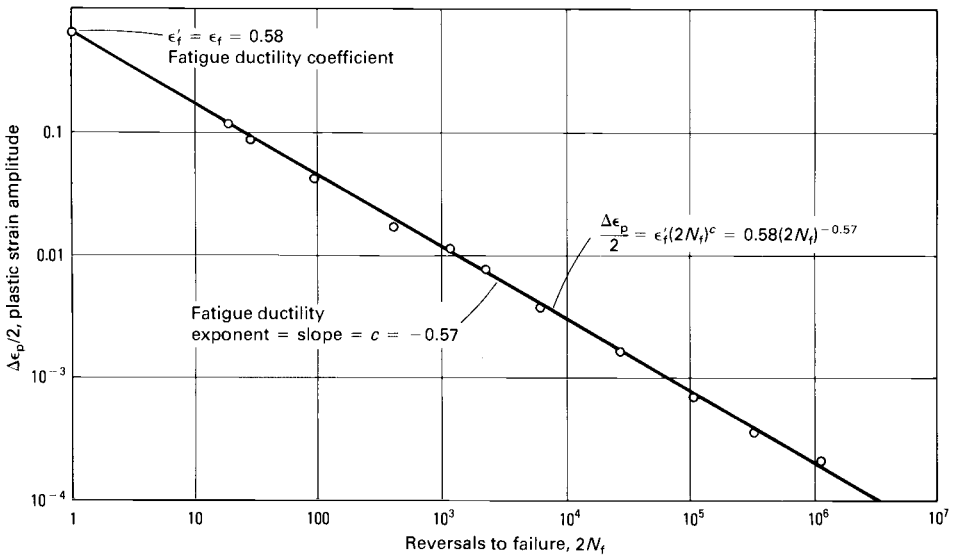

Fig. 10 Ductility versus fatigue life for annealed AISI-SAE 4340 steel. Source: Ref 8

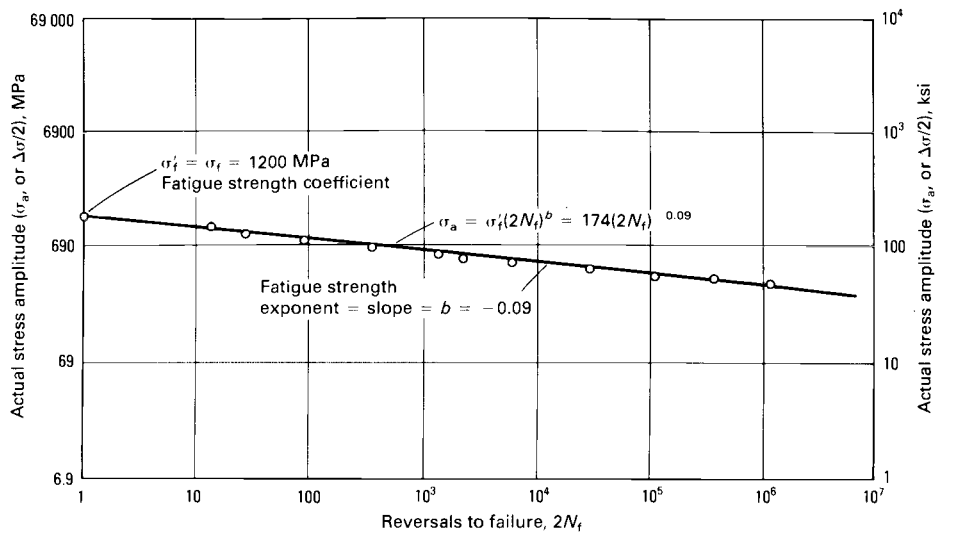

Fig. 11 Strength versus fatigue life for annealed AISI-SAE 4340 steel. The equation for the actual stress amplitude, σ_a, is shown in ksi units. Source: Ref 8

The total strain range is the sum of the elastic and plastic components, obtained by adding Eq 6 and 8 (see Fig. 12):

$$\frac{\Delta\epsilon}{2} = \epsilon_f'(2N_f)^c + \frac{\sigma_f'}{E}(2N_f)^b \qquad \text{(Eq 9)}$$

For low-cycle fatigue conditions (frequently fewer than about 1000 cycles to failure), the first term of Eq 9 is much larger than the second; thus, analysis and design under such conditions must use the strain-based approach. For long-life fatigue conditions (frequently more than about 10 000 cycles to failure), the second term dominates, and the fatigue behavior is adequately described by Eq 7. Thus, it becomes possible to use Eq 7 in stress-based analysis and design.

Figure 13 shows the fatigue life behavior of two high-strength plate steels for which extensive fatigue data exist. ASTM A 440 has a yield strength of about 345 MPa (50 ksi); the other steel is a proprietary grade hardened and tempered to a yield strength of about 750 MPa (110 ksi). Under long-life fatigue conditions, the higher-strength steel can accommodate higher strain amplitudes for any specified number of cycles; such strains are elastic. Thus, stress and strain are proportional, and it is apparent that the higher-strength steel has a higher fatigue limit. With low-cycle fatigue conditions, however, the more ductile lower-strength steel can accommodate higher strain amplitudes. For low-cycle fatigue conditions (in which the yield strength of the material is exceeded on every cycle), the lower-strength steel can accommodate more strain reversals before failure for a specified strain amplitude. For strain amplitudes of 0.003 to 0.01, the two steels have the same fatigue life, 10^4 to 10^5 cycles. For this particular strain amplitude, most steels have the same fatigue life, regardless of their strength levels. Heat treating a steel to different hardness levels does not appreciably change the fatigue life for this strain amplitude (Fig. 14).

Fuchs and Stephens's text (Ref 9), *Proceedings of the SAE Fatigue Conference* (Ref 10), and the recently published update to the SAE *Fatigue Design Handbook* (Ref 11) provide much additional detail on the use of state-of-the-art fatigue analysis methods. In fact, the chapter outline for the latter work, shown in Fig. 15, provides an excellent checklist of factors to include in a fatigue analysis.

Metallurgical Variables of Fatigue Behavior

The metallurgical variables having the most pronounced effects on the fatigue behavior of carbon and low-alloy steels are strength level, ductility, cleanliness of the steel, residual stresses, surface conditions, and aggressive environments. At least partly because of the characteristic scatter of fatigue testing data, it is difficult to distinguish the direct effects of other variables such as composition on fatigue from their effects on the strength level of steel. Reference 3 addresses some excellent research in the area of microstructure and its effect on fatigue.

Strength Level. For most steels with hardnesses below 400 HB (not including precipitation hardening steels), the fatigue limit is about half the ultimate tensile strength. Thus, any heat treatment or alloying addition that increases the strength (or hardness) of a steel can be expected to increase its fatigue limit as shown in Fig. 5 for a low-alloy steel (AISI 4340) and in Fig. 16 for various other low-alloy steels as a function of hardness. However, as shown in Fig. 14 for medium-carbon steel, a higher hardness (or strength) may not be associated with improved fatigue behavior in a low-cycle regime ($<10^3$ cycles) because ductility may be a more important factor.

Ductility is generally important to fatigue life only under low-cycle fatigue conditions. Exceptions to this include spectrum loading where there is an occasional overload with millions of smaller cycles, or extremely brittle materials where crack propagation dominates. The fatigue-ductility coefficient, ϵ_f', can be estimated from the reduction in area occurring in a tension test.

Cleanliness of a steel refers to its relative freedom from nonmetallic inclusions. These inclusions generally have a deleterious effect on the fatigue behavior of steels, particularly for long-life applications. The type, number, size, and distribution of nonmetallic inclusions may have a greater effect on the fatigue life of carbon and alloy steel than will differences in composition, microstructure, or stress gradients. Nonmetallic inclu-

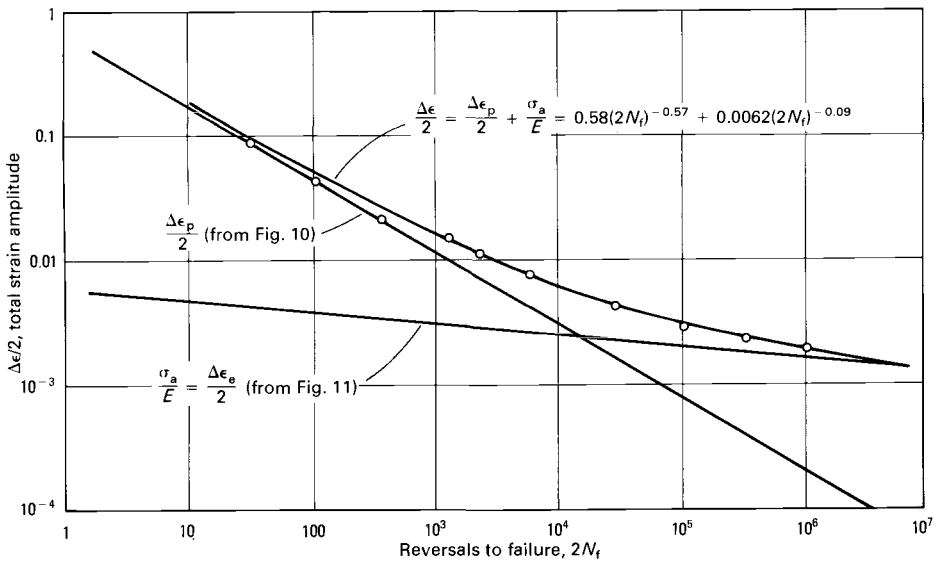

Fig. 12 Total strain versus fatigue life for annealed AISI-SAE 4340 steel. Data are same as in Fig. 10 and 11. Source: Ref 8

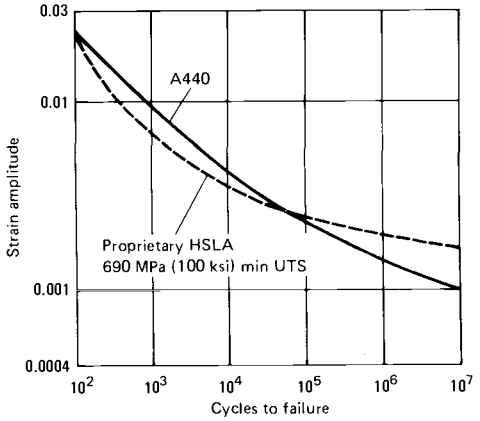

Fig. 13 Total strain versus fatigue life for two high-strength low-alloy (HSLA) steels. Steels are ASTM A 440 having a yield strength of about 345 MPa (50 ksi) and a proprietary quenched and tempered HSLA steel having a yield strength of about 750 MPa (110 ksi). Source: Ref 7

sions, however, are rarely the prime cause of the fatigue failure of production parts; if the design fatigue properties were determined using specimens containing inclusions representative of those in the parts, any effects of these inclusions would already be incorporated in the test results. Great care must be used when rating the cleanliness of a steel based on metallographic examination to ensure that the limited sample size (volume rated) is representative of the critical area in the final component.

Points on the lower curve in Fig. 17 represent the cycles to failure for a few specimens from one bar selected from a lot consisting of several bars of 4340H steel. Large spherical inclusions, about 0.13 mm (0.005 in.) in diameter, were observed in the fracture surfaces of these specimens. The inclusions were identified as silicate particles. No spherical inclusions larger than 0.02 mm (0.00075 in.) were detected in the other specimens.

Large nonmetallic inclusions can often be detected by nondestructive inspection; steels can be selected on the basis of such inspection. Vacuum melting, which reduces the number and size of nonmetallic inclusions, increases the fatigue limit of 4340 steel, as can be seen in Table 2. Improvement in fatigue limit is especially evident in the transverse direction.

Surface conditions of a metal part, particularly surface imperfections and roughness, can reduce the fatigue limit of the part. This effect is most apparent for high-strength steels. The interrelationship between surface roughness, method of producing the surface finish, strength level, and fatigue limit is shown in Fig. 8, in which the ordinate represents the fraction of fatigue limit relative to a polished test specimen that could be anticipated for the combination of strength level and surface finish.

Fretting is a wear phenomenon that occurs between two mating surfaces. It is adhesive in nature, and vibration is its essential causative factor. Usually, fretting is accompanied by oxidation. Fretting usually occurs between two tight-fitting surfaces that are subjected to a cyclic, relative motion of extremely small amplitude. Fretted regions are highly sensitive to fatigue cracking. Under fretting conditions, fatigue cracks are initiated at very low stresses, well below the fatigue limit of nonfretted specimens.

Decarburization is the depletion of carbon from the surface of a steel part. As indicated in Fig. 18, it significantly reduces the fatigue limits of steel. Decarburization of from 0.08 to 0.75 mm (0.003 to 0.030 in.)

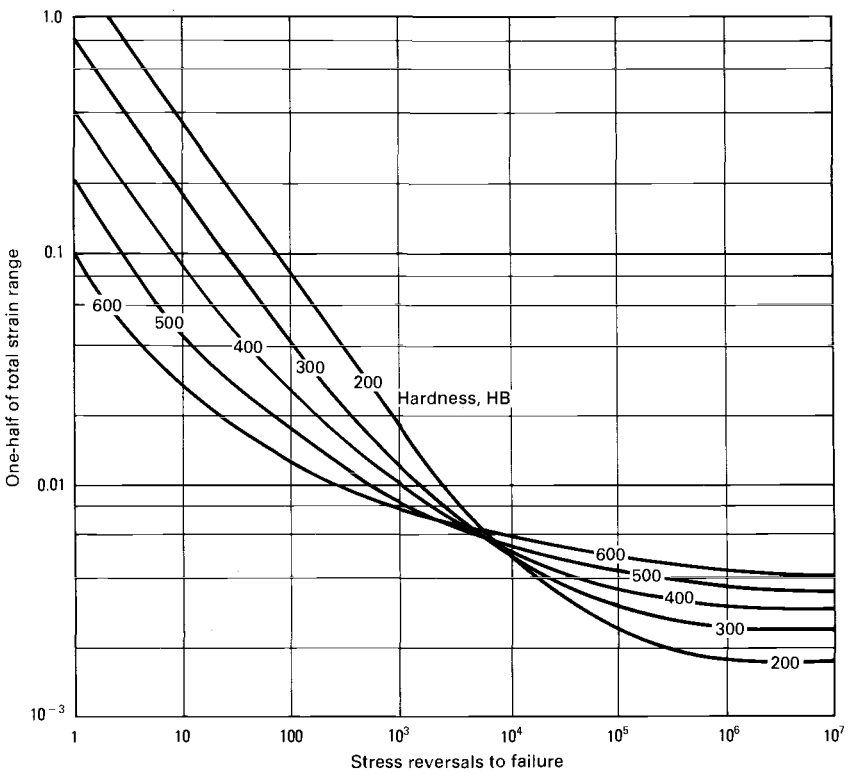

Fig. 14 Effect of hardness level on plot of total strain versus fatigue life. These are predicted plots for typical medium-carbon steel at the indicated hardness levels. The prediction methodology is described under the heading "Notches" in this article.

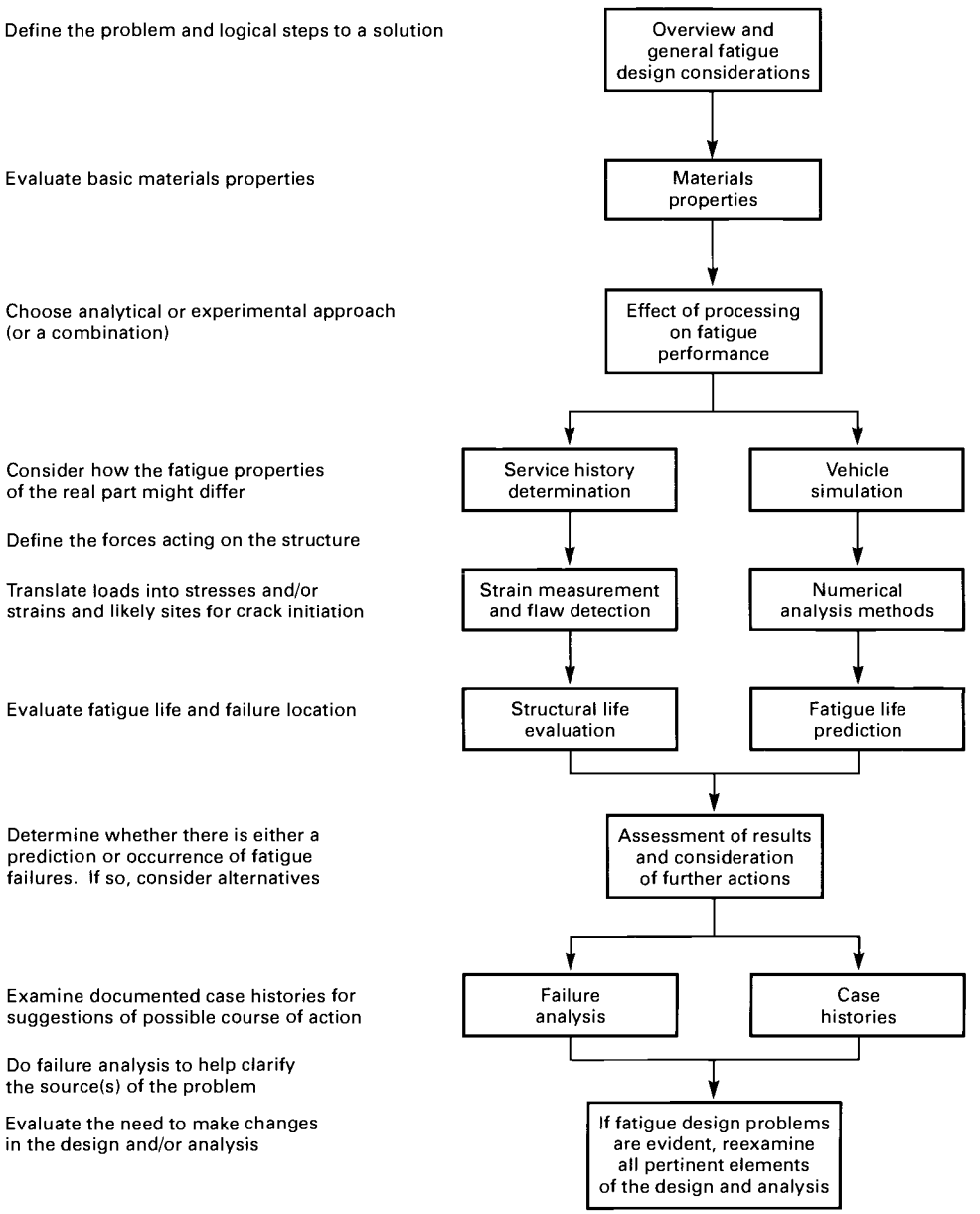

Fig. 15 Checklist of factors in fatigue analysis. Source: Ref 11

on AISI-SAE 4340 notched specimens that have been heat treated to a strength level of 1860 MPa (270 ksi) reduces the fatigue limit almost as much as a notch with $K_t = 3$.

When subjected to the same heat treatment as the core of the part, the decarburized surface layer is weaker and therefore less resistant to fatigue than the core. Hardening a part with a decarburized surface can also introduce residual tensile stresses, which reduce the fatigue limit of the material. Results of research studies have indicated that fatigue properties lost through decarburization can be at least partially regained by recarburization (carbon restoration in the surfaces).

Residual Stresses. The fatigue properties of a metal are significantly affected by the residual stresses in the metal. Compressive residual stresses at the surface of a part can improve its fatigue life; tensile residual stresses at the surface reduce fatigue life. Beneficial compressive residual stresses may be produced by surface alloying, surface hardening, mechanical (cold) working of the surface, or by a combination of these processes. In addition to introducing compressive residual stresses, each of these processes strengthens the surface layer of the material. Because most real components also receive significant bending and/or torsional loads, where the stress is highest at the surface, compressive surface stresses can provide significant benefit to fatigue.

Surface Alloying. Carburizing, carbonitriding, and nitriding are three processes for surface alloying. The techniques required to achieve these types of surface alloying are discussed in Volume 2 of the 8th Edition and Volume 4 of the 9th Edition of *Metals Handbook*. In these processes, carbon, nitrogen, or both elements are introduced into the surface layer of the steel part. The solute atoms strengthen the surface layer of the steel and increase its bulk relative to the metal below the surface. The case and core of a carburized steel part respond differently to the same heat treatment; because of its higher carbon content, the case is harder after quenching and harder after tempering. To achieve maximum effectiveness of surface alloying, the surface layer must be much thinner than the thickness of the part to maximize the effect of the residual stresses; however, the surface layer must be thick enough to prevent operating stresses from affecting the material just below the surface layer. Figure 19 shows the improvement in fatigue limit that can be achieved by nitriding. A particular advantage of surface alloying in the resistance to fatigue is that the alloyed layer closely follows the contours of the part.

Surface Hardening. Induction, flame, laser, and electron beam hardening selectively harden the surface of a steel part; the steel must contain sufficient carbon to permit hardening. In each operation, the surface of the part is rapidly heated, and the part is quenched either by externally applied quenchant or by internal mass effect. This treatment forms a surface layer of martensite that is bulkier than the steel beneath it. Further information on these processes may be found in Volume 2 of the 8th Edition and Volume 4 of the 9th Edition of *Metals Handbook*. Induction, flame, laser, and electron beam hardening can produce beneficial surface residual stresses that are compressive; by comparison, surface residual stresses resulting from through hardening are often tensile. Figure 20 compares the fatigue life of through-hardened, carburized, and induction-hardened transmission shafts.

Figure 21 shows the importance of the proper case depth on fatigue life; the hardened case must be deep enough to prevent operating stresses from affecting the steel beneath the case. However, it should be thin enough to maximize the effectiveness of the residual stresses. Three advantages of induction, flame, laser, or electron beam hardening in the resistance of fatigue are:

- The core may be heat treated to any appropriate condition
- The processes produce relatively little distortion
- The part may be machined before heat treatment

Mechanical working of the surface of a steel part effectively increases the resistance to fatigue. Shot peening and skin rolling are two methods for developing com-

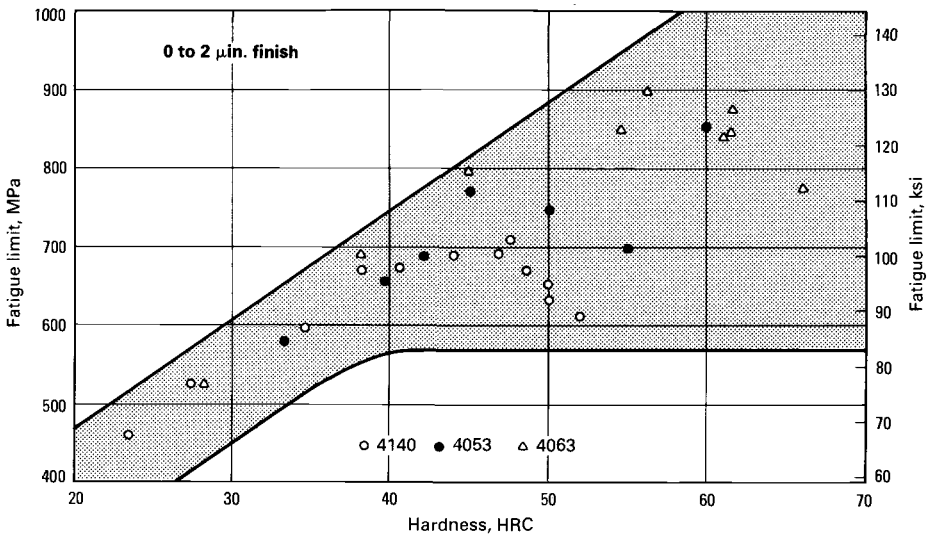

Fig. 16 Effect of carbon content and hardness on fatigue limit of through-hardened and tempered 4140, 4053, and 4063 steels. See the sections "Composition" and "Scatter of Data" in this article for additional discussions.

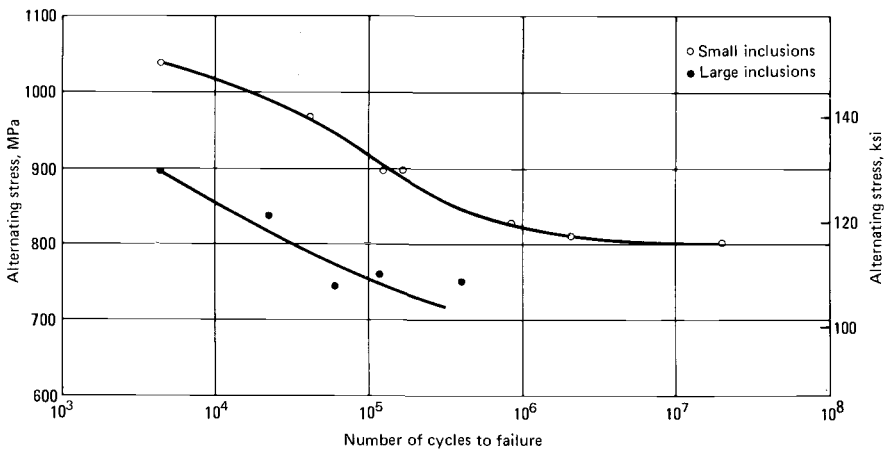

Fig. 17 Effect of nonmetallic inclusion size on fatigue. Steels were two lots of AISI-SAE 4340H; one lot (lower curve) contained abnormally large inclusions; the other lot (upper curve) contained small inclusions.

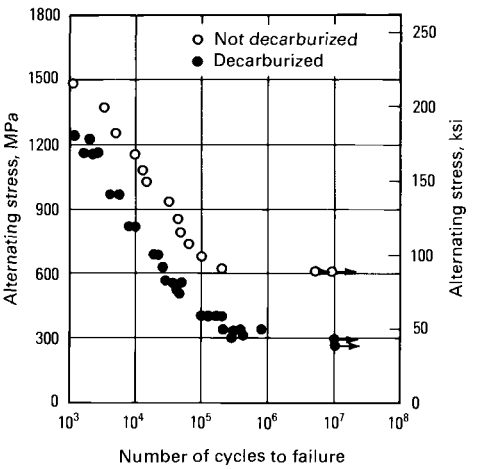

Fig. 18 Effect of decarburization on the fatigue behavior of a steel

pressive residual stresses at the surface of the part. The improvement in fatigue life of a crankshaft that results from shot peening is shown in Fig. 19. Shot peening is useful in recovering the fatigue resistance lost through decarburization of the surface. Decarburized specimens similar to those described in Fig. 18 were shot peened, raising the fatigue limit from 275 MPa (40 ksi) after decarburizing to 655 MPa (95 ksi) after shot peening.

Tensile residual stresses at the surface of a steel part can severely reduce its fatigue limit. Such residual stresses can be produced by through hardening, cold drawing, welding, or abusive grinding. For applications involving cyclic loading, parts containing these residual stresses should be given a stress relief anneal if feasible.

Aggressive environments can substantially reduce the fatigue life of steels. In the absence of the medium causing corrosion, a previously corroded surface can substantially reduce the fatigue life of the steel, as shown in Fig. 8. Additional information on corrosion fatigue is contained in Volumes 8 and 13 of the 9th Edition of *Metals Handbook*.

Grain size of steel influences fatigue behavior indirectly through its effect on the strength and fracture toughness of the steel. Fine-grained steels have greater fatigue strength than do coarse-grained steels.

Composition. An increase in carbon content can increase the fatigue limit of steels, particularly when the steels are hardened to 45 HRC or higher (Fig. 16). Other alloying elements may be required to attain the desired hardenability, but they generally have little effect on fatigue behavior.

Microstructure. For specimens having comparable strength levels, resistance to fatigue depends somewhat on microstructure. A tempered martensite structure provides the highest fatigue limit. However, if the structure as-quenched is not fully martensitic, the fatigue limit will be lower (Fig. 22). Pearlitic structures, particularly those with coarse pearlite, have poor resistance to fatigue. *S-N* curves for pearlitic and spheroidized structures in a eutectoid steel are shown in Fig. 23.

Macrostructure differences typical of those seen when comparing ingot cast to continuously cast steels can have an effect on fatigue performance. While there is no inherent difference between these two types of steel after rolling to a similar reduction in area from the cast ingot, bloom, or billet, ingot cast steels will typically receive much larger reductions in area (with subsequent refinement of grain size and inclusions) than will continuously cast billets when rolled to a constant size. Therefore, the billet size of continuously cast steels becomes important to fatigue, at least as it relates to the size of the material from which the part was fabricated.

A significant amount of research has shown that for typical structural applications, strand cast reduction ratios should be above 3:1 or 5:1, although many designers of critical forgings still insist on reduction ratios greater than 10:1 or 15:1. These larger reduction ratio requirements will frequently preclude the use of continuously cast steels because the required caster size would be larger than existing equipment. While this may not be a major problem at this time, steel trends suggest that there will be very little domestic and almost no off-shore ingot cast material available at any cost within the next two decades. The problem will be reduced as larger and larger casters, approaching bloom and ingot sizes, are installed.

Creep-Fatigue Interaction. At temperatures sufficiently elevated to produce creep, creep-fatigue interaction can be a factor affecting fatigue resistance. Information on creep-fatigue interaction is contained in the article "Elevated-Temperature Properties of Ferritic Steels" in this Volume.

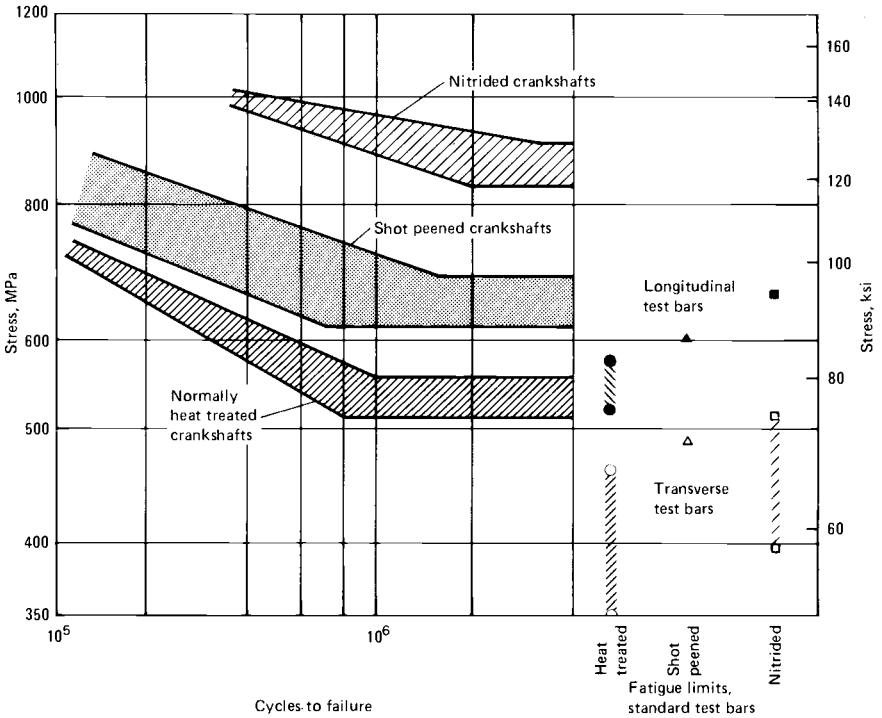

Fig. 19 Effect of nitriding and shot peening on fatigue behavior. Comparison between fatigue limits of crankshafts (*S-N* bands) and fatigue limits of separate test bars, which are indicated by plotted points at right. Steel was 4340.

Table 2 Improvement in the fatigue limits of SAE 4340 steel with the reduction of nonmetallic inclusions by vacuum melting compared to electric furnace melting

	Longitudinal fatigue limit(a)		Transverse fatigue limit(a)		Ratio of transverse to longitudinal	Hardness, HRC
	MPa	ksi	MPa	ksi		
Electric furnace melted	800	116	545	79	0.68	27
Vacuum melted	960	139	825	120	0.86	29

(a) Determined in repeated bending fatigue test ($R = 0$). Source: Ref 12

The orientation of cyclic stress relative to the fiber axis or rolling direction of a steel can affect the fatigue limit of the steel. Figure 24 shows the difference between the fatigue limit of specimens taken parallel to the rolling direction and those taken transverse to it. Any nonmetallic inclusions present will be elongated in the rolling direction and will reduce fatigue life in the transverse direction. The use of vacuum melting to reduce the number and size of nonmetallic inclusions therefore can have a beneficial effect on transverse fatigue resistance (Table 2).

Application of Fatigue Data

The application of fatigue data in engineering design is complicated by the characteristic scatter of fatigue data; variations in surface conditions of actual parts; variations in manufacturing processes such as bending, forming, and welding; and the uncertainty of environmental and loading conditions in service. In spite of the scatter of fatigue data, it is possible to estimate service life under cyclic loading. It is essential to view such estimates for what they are, that is, estimates of the mean or average performance, and to recognize that there may be large discrepancies between the estimated and actual service lives.

Scatter of Data. Fatigue testing of test specimens and actual machine components produces a wide scatter of experimental results (see Fig. 25 and Ref 10 for examples). The data in Fig. 25 represent fatigue life simulated-service testing of 25 lots of 12 torsion bars each. In this program, the coefficient of variation, C_N, defined as the ratio of the standard deviation of the mean value, of fatigue life was 0.28. In Table 3, the range of values of the coefficient of variation for fatigue strength is compared with those for other mechanical properties.

For specimens tested near the fatigue limit, the probable range of fatigue life becomes so large that it is pointless to compute a coefficient of variation for fatigue life. Instead, values of C_N are calculated for the fatigue limit. Approximately 1000 fatigue specimens were made from a single heat of aircraft quality 4340 steel; all were taken parallel to the fiber axis of the steel. The specimens were heat treated to three different strength levels and polished to a surface roughness of 0 to 0.050 μm (0 to 2 μin.). Fatigue limits for these specimens are given in terms of the percent surviving 10 million cycles (Fig. 26). It should be noted that the scatter increases as the strength level is increased; a similar trend is shown in Fig. 16.

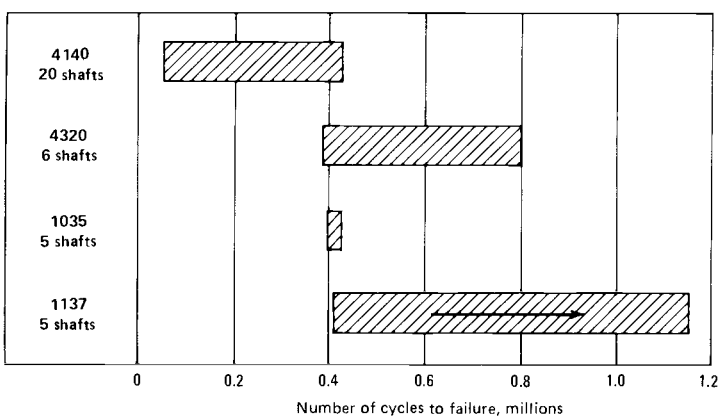

Steel	Surface hardness, HRC	Hardening process
4140	36–42	Through hardened
4320	40–46	Carburized to 1.0–1.3 m (0.040–0.050 in.)
1035	42–48	Induction hardened to 3 mm (0.120 in.) min effective depth (40 HRC)
1137	42–48	Induction hardened to 3 mm (0.120 in.) min effective depth (40 HRC)

Fig. 20 Effect of carburizing and surface hardening on fatigue life. Comparison of carburized, through-hardened, and induction-hardened transmission shafts tested in torsion. Arrow in lower bar on chart indicates that one shaft had not failed after the test was stopped at the number of cycles shown.

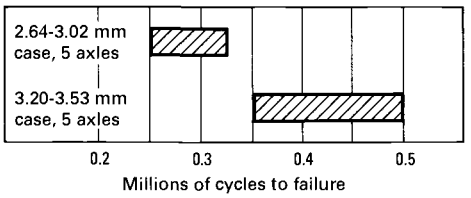

Fig. 21 Effect of case depth on fatigue life. Fatigue tests on induction-hardened 1038 steel automobile axle shafts 32 mm (1¼ in.) in diameter. Case depth ranges given on the chart are depths to 40 HRC. Shafts with lower fatigue life had a total case depth to 20 HRC of 4.5 to 5.2 mm (0.176 to 0.206 in.), and shafts with higher fatigue life, 6.4 to 7.0 mm (0.253 to 0.274 in.). Load in torsion fatigue was 2030 N · m (1500 ft · lbf), and surface hardness was 58 to 60 HRC after hardening.

Variation from heat to heat with the same steel is greater than variation within a single heat. Figure 27 shows the variations in fatigue limit among five heats of 8740 steel; all specimens were hardened and tempered to 39 HRC. Specimens taken from heat E were given a variety of heat treatments, all of which resulted in a hardness of 39 HRC. The variations in fatigue limit resulting from these heat treatments are also shown in Fig. 27.

Additional scatter of fatigue data is likely to result from variations in case depth, surface finish, dimensions of the part or specimen, or environmental or residual stresses. Axial load tests for fatigue properties are considered more conservative than rotating bending tests but have the advantage of obtaining information on fatigue properties at various mean stresses.

Estimating Fatigue Parameters. In the strain-based approach to fatigue, five parameters (σ_f', b, ϵ_f', c, and E) are used to describe fatigue behavior. These parameters can be determined experimentally; typical values (which should not be considered averages or minimums) obtained for several materials are given in Table 4. In the absence of experimentally determined values, these parameters have been estimated from uniaxial tension test results. The use of these parameters (either experimentally determined or estimated values) to predict fatigue behavior only approximates actual behavior and should never be substituted for full-scale testing of actual parts under service conditions.

Table 3 Coefficients of variation for mechanical properties

Mechanical property	Coefficient of variation, (C_n)(a)
Elastic modulus	0.03
Ultimate tensile strength	0.05
Brinell hardness	0.05
Tensile yield strength	0.07
Fracture toughness	0.07
Fatigue strength	0.08 to 1.0

(a) Coefficient of variation, C_n, is the standard deviation divided by the mean value. Source: Ref 12

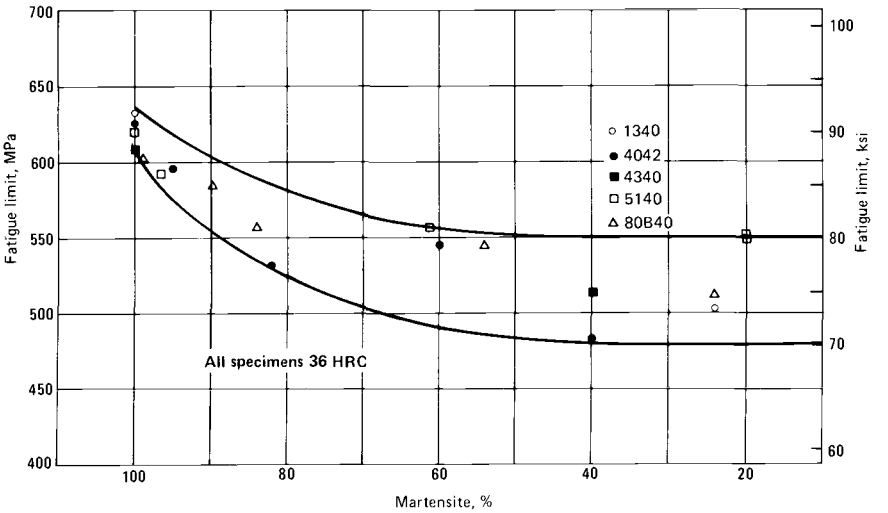

Fig. 22 Effect of martensite content on fatigue limit. Data are based on standard rotating-beam fatigue specimens of alloy steels 6.3 mm (0.250 in.) in diameter with polished surfaces.

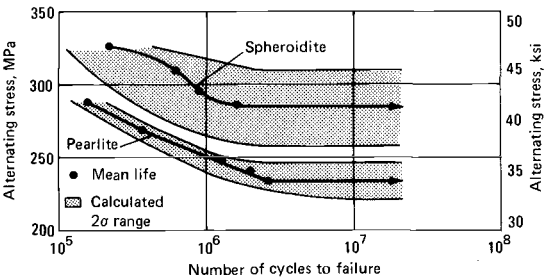

Property	Spheroidite	Pearlite
Tensile strength, MPa (ksi)	641 (93)	676 (98)
Yield strength, MPa (ksi)	490 (71)(a)	248 (36)(b)
Elongation in 50 mm (2 in.), %	28.9	17.8
Reduction in area, %	57.7	25.8
Hardness, HB	92	89

(a) Lower yield point. (b) 0.1% offset yield strength

Fig. 23 Effect of microstructure on fatigue behavior of carbon steel (0.78% C, 0.27% Mn, 0.22% Si, 0.016% S, and 0.011% P)

As described earlier, the fatigue strength coefficient, σ_f', is the intercept of the true stress amplitude-fatigue life plot at one reversal. The fatigue strength exponent, b, is the slope (always negative) of this line.

For steels with hardnesses below 500 HB, σ_f' may be approximated by:

$$\sigma_f' = S_u + 345 \quad \text{(Eq 10a)}$$

where σ_f' and S_u, the ultimate tensile strength, are given in MPa, or by:

$$\sigma_f' = S_u + 50 \quad \text{(Eq 10b)}$$

where σ_f' and S_u are given in ksi. If the tensile strength is not known, it may be approximated at 3.4 MPa (500 psi) times the Brinell hardness number.

The value of the fatigue strength exponent, b, is usually about −0.085. If the steel has been fully annealed, the value of b may be as high as −0.1. If the steel has been severely cold worked, the value of b may be as low as −0.05.

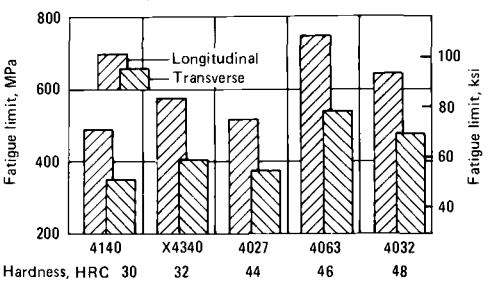

Steel	No. of tests(a)	Average tensile strength, MPa (ksi)	Hardness, HRC
Longitudinal tests			
4027	11	1179 (171)	37–39
4063	12	1682 (244)	47–48
4032	11	1627 (236)	46–48
Transverse tests			
4027	10	1130 (164)	34–39.5
4063	9	1682 (244)	47–48.5
4032	10	1254 (182)	47.5–48.5

(a) Number of fatigue specimens. For 4140 steel, 50 longitudinal and 50 transverse specimens were tested: for 4340 steel, 10 longitudinal and 10 transverse specimens were used.

Fig. 24 Effect of specimen orientation on fatigue limit. Orientations are relative to the fiber axis resulting from hot working on the fatigue limit of low-alloy steels. Through-hardened and tempered specimens, 6.3 mm (0.250 in.) in diameter, were taken from production billets. Specimens for each grade were from the same heat of steel, but the tensile and fatigue specimens were heat treated separately, accounting for one discrepancy in hardness readings between the chart and the tabulation above. Fatigue limit is for 100 × 10^6 cycles.

Table 4 Cyclic and monotonic properties of selected as-received and heat-treated steels

For a more complete, up-to-date listing of cyclic-fatigue properties, see Ref 13.

SAE steel			Ultimate tensile strength			Modulus of elasticity		Yield strength		Cyclic strain hardening
Grade	Brinell hardness, HB	Condition(a)	MPa	ksi	Reduction in area, %	GPa	10^6 psi	MPa	ksi	exponent
1006	85	As-received	318	46.1	73	206	30	224	32.5	0.21
1018	106	As-received	354	51.3		200	29	236	34.2	0.27
1020	108	As-received	392	56.9	64	186	27	233	33.8	0.26
1030	128	As-received	454	65.8	59	206	30	248	36	0.29
1035	...	As-received	476	69.0	56	196	28.4	270	39	0.24
1045	...	As-received	671	97.3	44	216	31.3	353	51.2	0.22
1045	390	QT	1343	194.8	59	206	30	842	122	0.09
1045	450	QT	1584	229.7	55	206	30	1069	155	0.09
1045	500	QT	1825	265	51	206	30	1259	182.6	0.12
1045	595	QT	2240	325	41	206	30	1846	267.7	0.10
4142	380	QT	1412	205	48	206	30	966	140	0.14
4142	450	QT	1757	255	42	206	30	1160	168	0.11
4142	670	QT	2445	355	6	200	29	2238	324.6	0.07
4340	242	As-received	825	120	43	192	27.8	467	67.7	0.17
4340	409	QT	1467	213	38	200	29	876	127	0.13
SAE 950X	...	As-rolled	438	63.5	64	206	30	339	49.2	0.14
SAE 960X	...	As-rolled	480	70	...	206	30	417	60.5	0.14
SAE 980X	...	As-rolled	652	94.6	75	206	30	514	74.5	0.13

SAE steel		Cyclic strength coefficient		Fatigue strength coefficient (σ_f')		Fatigue strength exponent (b)	Fatigue ductility coefficient, ϵ_f'	Fatigue ductility exponent (c)
Grade	Brinell hardness, HB	MPa	ksi	MPa	ksi			
1006	85	813	118	756	109.6	−0.13	1.22	−0.67
1018	106	1259	182.6	782	113.4	−0.11	0.19	−0.41
1020	108	1206	175	850	123.2	−0.12	0.44	−0.51
1030	128	1545	224	902	130.8	−0.12	0.17	−0.42
1035	...	1185	172	906	131.4	−0.11	0.33	−0.47
1045	...	1402	203.3	1099	159.4	−0.11	0.52	−0.54
1045	390	1492	216.4	1408	204.2	−0.07	1.51	−0.85
1045	450	1874	271.8	1686	244.5	−0.06	0.97	−0.83
1045	500	2636	382.3	2165	314	−0.08	0.22	−0.66
1045	595	3498	507.3	3047	441.9	−0.10	0.13	−0.79
4142	380	2259	327.6	1820	264	−0.08	0.65	−0.76
4142	450	2359	342.1	2017	292.5	−0.08	0.85	−0.90
4142	670	3484	505.3	2727	395.5	−0.08	0.06	−1.47
4340	242	1384	200.7	1232	178.7	−0.10	0.53	−0.56
4340	409	1950	283	1898	275.3	−0.09	0.67	−0.64
SAE 950X	...	796	115.4	800	116	−0.10	1.23	−0.62
SAE 960X	...	969	140.5	895	130	−0.09	0.46	−0.65
SAE 980X	...	1135	164.6	1146	166.2	−0.09	1.10	−0.72

(a) QT, quenched and tempered. Source: Ref 10

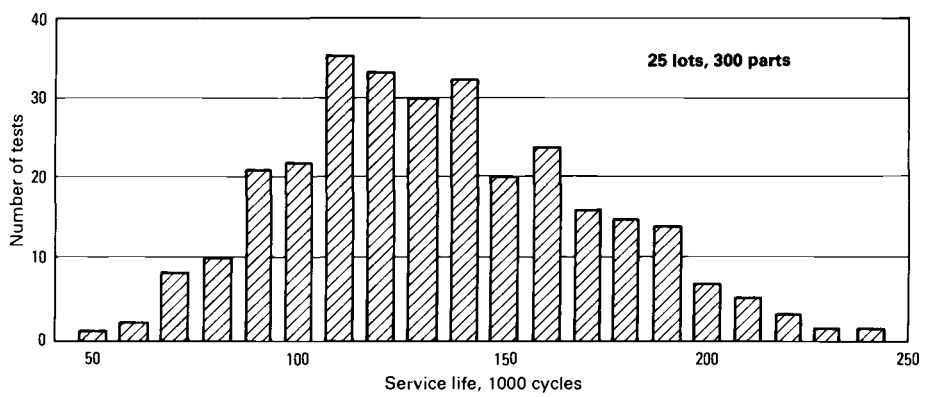

Fig. 25 Distribution of fatigue lifetimes from simulated service fatigue tests of front suspension torsion bar springs of 5160H steel. Size of hexagonal bar section was 32 mm (1.25 in.); mean service life, 134 000 cycles; standard deviation, 37 000 cycles; coefficient of variations, 0.28.

For a fatigue life of more than a million cycles, the use of these parameters in Eq 7 provides a slightly lower estimate of fatigue limit than the frequently used rule of thumb that the fatigue limit is half the ultimate tensile strength.

The fatigue ductility coefficient, ϵ_f', is approximated by the true fracture ductility, ϵ_f, which can be calculated from the reduction in area in a tension test by:

$$\epsilon_f' \approx \epsilon_f = \ln\left(\frac{100}{100 - \%RA}\right) \qquad \text{(Eq 11)}$$

If the reduction in area (% RA) can be estimated from hardness levels, typical values of ϵ_f' can then be approximated by the use of Eq 11. For example:

- With hardness less than 200 HB, RA is approximately 65%, and $\epsilon_f' = 1.0$
- With hardness between 200 and 300 HB, RA is approximately 40%, and $\epsilon_f' = 0.5$
- With hardness greater than 400 HB, RA is approximately 10%, and $\epsilon_f' = 0.1$

The fatigue-ductility coefficient, ϵ_f', should be estimated from a measured percent of RA rather than obtained by using these approximate values, if possible.

The fatigue-ductility exponent, c, has approximately the same value (−0.6) for most ductile steels. Severe cold working may raise the value of c to −0.7; annealing or tempering at a high temperature may reduce c to about −0.5.

The elastic modulus (Young's modulus), E, is the slope of the elastic portion of the uniaxial stress-strain curve. For most steels, it has a value of about 200 GPa (29×10^6 psi). Further information on estimating these fatigue parameters may be found in Ref 10. As a check on estimating, the results should be compared with the data for a similar material in Table 4.

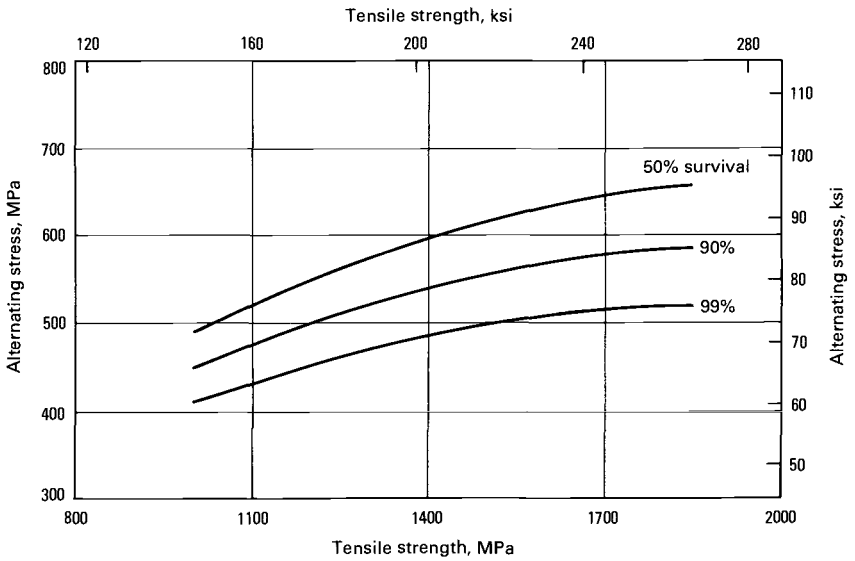

Fig. 26 Scatter of fatigue limit data. Based on the survival after 10 million cycles of approximately 1000 specimens, at one heat, of AISI-SAE 4340 steel with tensile strengths of 995, 1320, and 1840 MPa (144, 191, and 267 ksi). Rotating-beam fatigue specimens tested at 10 000 to 11 000 rev/min. Coefficients of variation, C_N, range from 0.17 to 0.20.

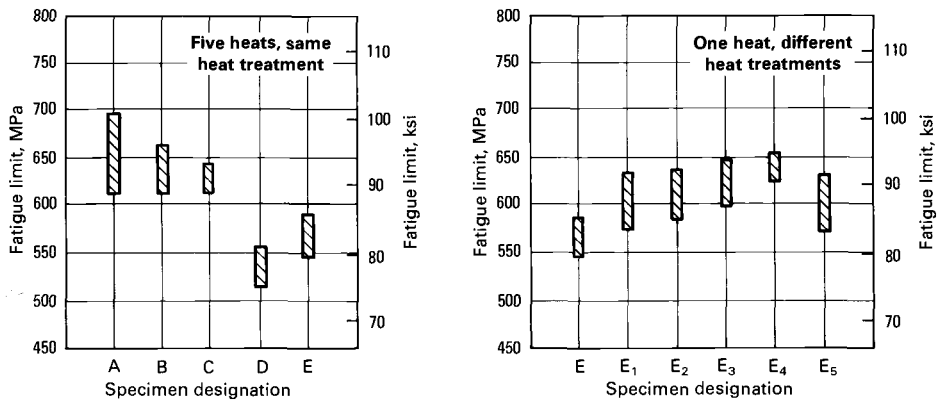

Specimen(a)	Hardness, HRC	Tensile strength MPa	Tensile strength ksi	Yield strength MPa	Yield strength ksi	Elongation in 50 mm (2 in.), %	Reduction of area, %
Five heats, same heat treatment							
A	39.1	1250	181	1205	175	14.7	56.0
B	39.3	1225	178	1185	172	15.3	56.7
C	38.2	1235	179	1185	172	15.3	52.3
D	39.1	1235	179	1170	170	15.0	55.0
E	39.7	1270	184	1220	177	13.7	55.3
One heat, different heat treatments to produce the same hardness							
E	39.7	1270	184	1220	177	13.7	55.3
E_1(b)	40.3	1260	183	1250	181	13.0	55.7
E_2(c)	39.3	1270	184	1210	176	14.3	54.3
E_3(d)	38.7	1270	184	1220	177	15.7	54.3
E_4(e)	39.0	1275	185	1230	178	14.3	55.3
E_5(f)	37.8	1230	178	1170	170	14.7	58.3

(a) The letters A, B, C, D, and E indicate different heats of 8740 steel. Specimens were normalized at 900 °C (1650 °F) 1 h and air cooled; austenitized at 825 °C (1520 °F) 1 h and oil quenched; tempered 2 h. (b) Austenitized at 815 °C (1500 °F) ½ h and oil quenched; tempered 2 h. (c) Normalized at 900 °C (1650 °F) 1 h and air cooled; austenitized at 840 °C (1540 °F) 1¼ h and oil quenched; tempered 2 h. (d) Normalized at 900 °C (1650 °F) 1 h and air cooled; austenitized at 815 °C (1500 °F) ½ h and oil quenched; tempered 2 h. (e) Austenitized at 840 °C (1540 °F) 1¼ h and oil quenched; tempered 2 h. (f) Homogenized at 1150 °C (2100 °F) 24 h and air cooled; normalized at 900 °C (1650 °F) 1 hr and air cooled; austenitized at 825 °C (1520 °F) 1 h and oil quenched; tempered 2 h

Fig. 27 Variations in fatigue limit for different heats and heat treatments

Estimating Fatigue Life. Designers of machine components to be subjected to cyclic loading would like to be able to predict the fatigue life from basic materials parameters and anticipated loading patterns. However, the scatter of fatigue data is so great that the likelihood of accurate predictions is extremely low. The methods and approximations in this article and in Ref 10, 11, and 13 to 15 can provide some indication of fatigue life. Efforts to estimate fatigue life when service temperatures make creep-fatigue interaction a factor are discussed in the article "Elevated-Temperature Properties of Ferritic Steels" in this Volume.

In a specific situation, the assessment of the seriousness of fatigue is aided by a knowledge of the cyclic strains involved in fatigue at various lives. Certain generalizations are useful guidelines for ductile steels:

- If the peak localized strains are completely reversed and the total range of strain is less than S_u/E, fatigue failures are likely to occur in a large number of cycles or not at all
- If the total strain range is greater than 2% (amplitude ± 1%), fatigue failure will probably occur in less than 1000 cycles
- Part configurations that prevent the use of the ductility of the metal and metals that have limited ductility are highly susceptible to fatigue failures

With respect to long-life fatigue, the relative magnitude of the change in fatigue strength due to processing may be crudely estimated by the relative changes produced in ultimate tensile strength and in hardness. If the ductility change is also measured and if the qualitative effects of various processes on different types of metal are known, more refined estimates of the change in fatigue behavior can be made without resorting to extensive fatigue testing.

Fatigue life may be estimated by inserting a calculated strain amplitude and the appropriate materials parameters from Table 4 into Eq 9 and then solving for the number of cycles to failure, N_f. Where deformation is purely elastic, a calculated stress amplitude and Eq 7 may be used. The calculated fatigue life must be adjusted to compensate for stress concentrations, surface finish, and the presence of aggressive environments, as described in Fig. 8 and Ref 6 to 11. Alternatively, the calculated stress may be adjusted by using stress concentration factors such as those in Ref 16 and 17. Any of these calculations includes the assumption that the loading is fully reversed ($R = -1$).

Potter (Ref 18) has described a method for approximating a constant-lifetime fatigue diagram for unnotched specimens. Using this method, a series of points corresponding to different lifetimes are calculated and plotted along a diagonal line for $R = -1$. Each of these points is connected by a straight line to the point on another diagonal ($R = 1.0$) that corresponds to the ultimate tensile strength. The calculated lines correspond well with the experimental lines. Generally, the predicted lines represent lower stresses than the actual data. Estimating fatigue parameters from

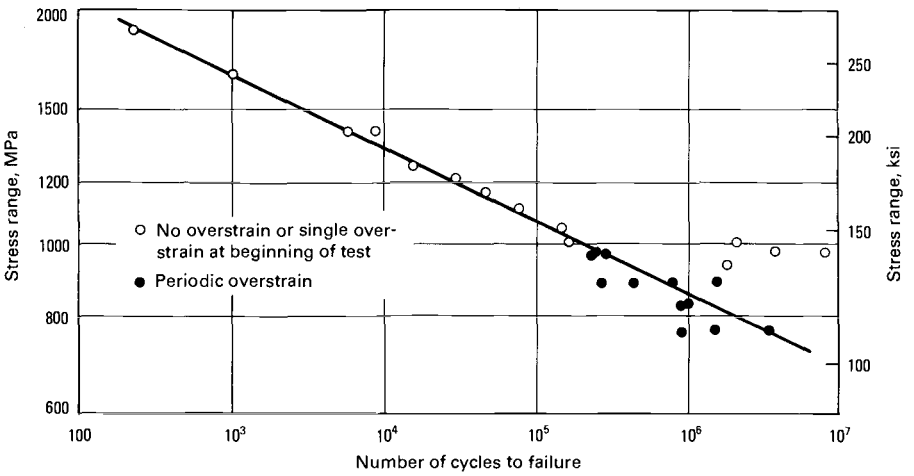

Fig. 28 Effect of overstrain on fatigue behavior. Shown here is the effect of periodic large strain cycles on the fatigue life of AISI-SAE 4340 steel hardened and tempered to a yield strength of 1100 MPa (160 ksi). Source: Ref 7

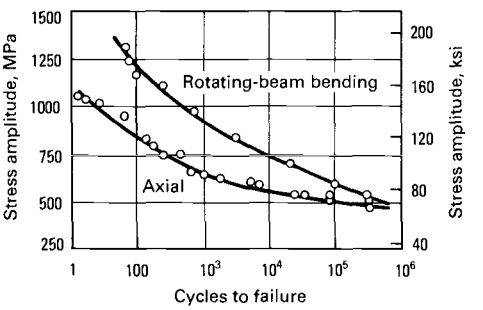

Fig. 29 Fatigue data under axial loading and rotating bending loading for 4340 steel. Source: Ref 21

the Brinell hardness number provides more conservative estimates. These results are only approximations, and the methods may not apply for every material.

While the likelihood of an accurate life prediction is relatively low, the use of these procedures is still valuable. There are very few "new" parts designed; most new parts are similar to a previously successful design, scaled up or down or operating at a slightly increased load. These procedures are very useful in estimating the change in life due to a change in design, load, processing, or material.

Cumulative Fatigue Damage. The data presented in this article, and most other published fatigue data, were obtained from constant-amplitude testing; all the load cycles in the test are identical. In actual service, however, the loading can vary widely during the lifetime of a part. There have been many approaches to evaluating the cumulative effects of variations in loading on the fatigue behavior of steels. References 7, 9, 10, 15, 18, and 19 describe methods of analyzing cumulative damage. A few overload cycles can reduce the fatigue life of steel, even though the mean load amplitude lies below the fatigue limit; this effect is shown in Fig. 28. The counting of each load cycle and the relative damage produced must be done with extreme accuracy and care. One method, rain flow counting (described in Ref 7, 9, 10, 15, 19, and 20), has been shown to be most effective. In this method, the cyclic stress-strain properties are applied such that the hysteresis behavior of the material (Fig. 9) is taken into account on each load excursion. Obviously, when there are millions of individual loads involved, the task becomes quite large. Frequently, a complex load or strain history will be simplified into a short block representing a fraction of the whole, and the damage in that block will be predicted. The block can then be repeated until failure, and component life can be predicted based on the fraction of the whole represented by the block. In any event, predicting fatigue behavior under these circumstances is difficult.

Notches. Fatigue failures in service nearly always start at the roots of notches. Because notches cannot always be avoided in design (though they should be avoided whenever possible), some allowance for notches must be made in calculating nominal stresses during the design process. A fatigue notch factor, K_f, should be introduced into the fatigue life calculations that use Eq 7:

$$S_a = \frac{\sigma_a}{K_f} = \frac{\sigma_f'}{K_f}(2N_f)^b \qquad \text{(Eq 12)}$$

where σ_a is the amplitude of the true stress.

The appropriate value of K_f depends on the shape of the notch, fatigue strength, ductility of the metal, residual stress, and design life of the part. Its value varies between 1 (no notch effect) and the theoretical stress concentration factor, K_t. References 16 and 17 list many useful stress concentration factors.

First estimates of notched fatigue performance may be based on $K_f = K_t$, especially for moderately notched, heat-treated steel parts that are expected to withstand many cycles. A value of $K_f < K_t$ can be used if a more exact value of K_f is available.

For notched parts, the value of K_f may be estimated from the equation:

$$K_f = 1 + \frac{K_t - 1}{1 + a/r} \qquad \text{(Eq 13)}$$

where r is the notch root radius; a is the material constant depending on strength and ductility.

For heat-treated steel, the following equation may be used to estimate a:

$$a = 0.025\left(\frac{2070}{S_u}\right)^{1.8} \qquad \text{(Eq 14a)}$$

where a is given in millimeters and the ultimate tensile strength, S_u, is given in MPa. For steels, values of a range from 0.064 to 0.25 mm. Values of a may also be estimated by using the equation:

$$a = \left(\frac{300}{S_u}\right)^{1.8} \times 10^{-3} \qquad \text{(Eq 14b)}$$

where a is given in inches and S_u in ksi.

When the required design life is relatively short, the effect of the notch will be even less than indicated by Eq 13 because of the large amount of inelastic strain at the root of the notch.

At low fatigue lives, a notch must be regarded as a strain concentration as well as a stress concentration. The product of the strain concentration factor, K_ϵ, and the stress concentration factor, K_σ, is equal to the square of the theoretical stress concentration factor:

$$K_\epsilon K_\sigma = (K_t)^2 \qquad \text{(Eq 15)}$$

At long lives, the behavior is nominally elastic so that K_ϵ equals K_σ, and both K_ϵ and K_σ are equal to K_t. At short lives, where K_σ is nominally 1, the strain concentration factor is equal to $(K_t)^2$. Usually, however, K_t is replaced by an effective value of K_f, as in Eq 12. This relation may be rewritten as:

$$(K_f \times \Delta S)^2 = \sigma_a \epsilon_a E \qquad \text{(Eq 16)}$$

where ΔS is the nominal calculated stress amplitude remote from the stress raiser, σ_a is the amplitude of the true stress (Eq 12), and ϵ_a is the amplitude of the true strain. The value of ϵ_a calculated can be used directly on a fatigue life diagram, such as Fig. 14, to estimate the fatigue life of an actual part.

Mean stresses may be introduced into the above equations by substituting the quantity $(\sigma_f - \sigma_0)$ for σ_f wherever it appears. Mean stresses affect fatigue behavior by increasing the amount of plastic strain whenever the algebraic sum of the mean and alternating stresses exceeds the yield strength.

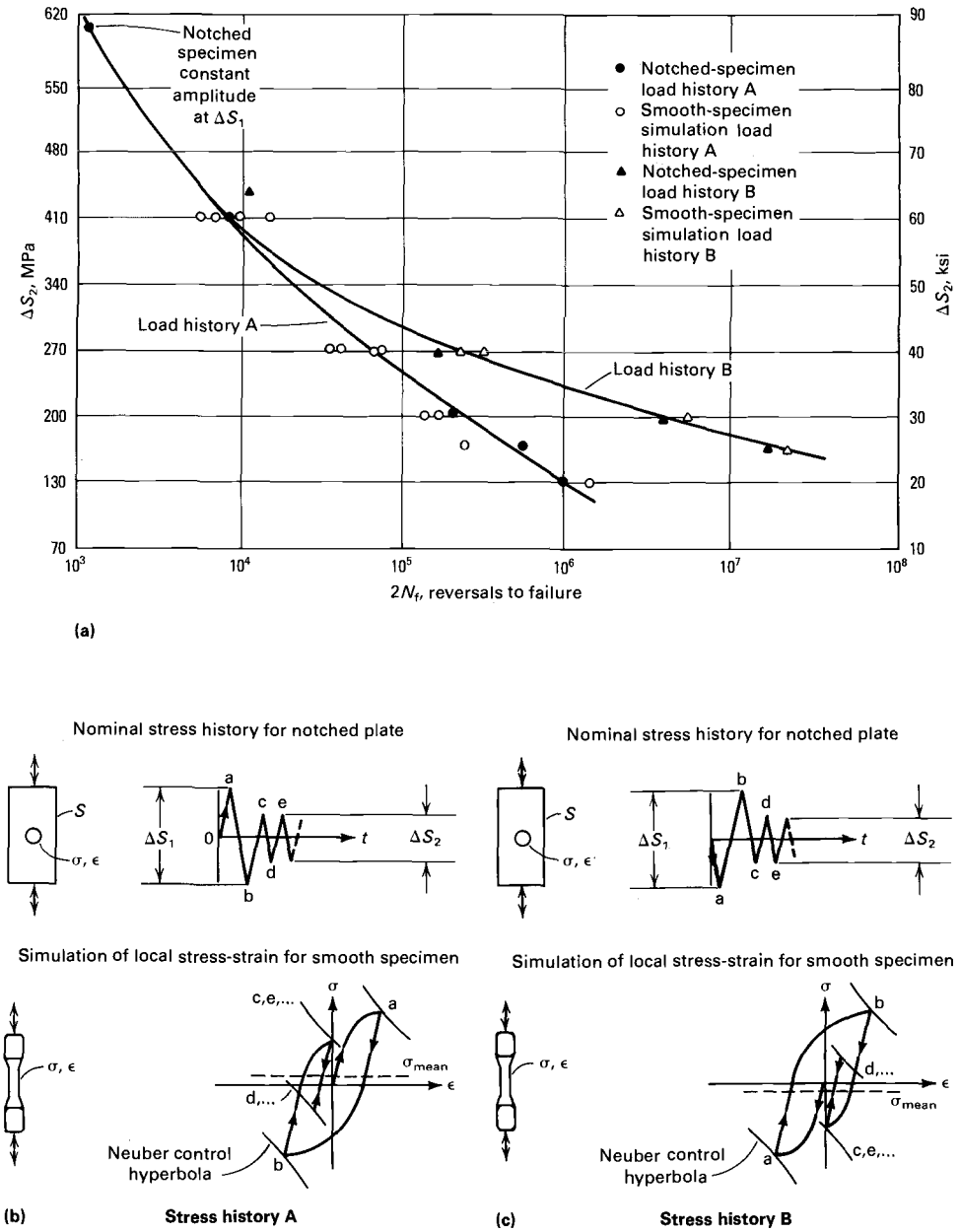

Fig. 30 Fatigue data (a) showing sequence effects for notched-specimen and smooth-specimen simulations (2024-T4 aluminum, $K_f = 2.0$). Load histories A and B have a similar cyclic load pattern (ΔS_2) but have slightly different initial transients (ΔS_1) with either (b) a tensile leading edge (first stress peak at $+\Delta S_1/2$) or (c) a compressive leading edge (first stress peak at $-\Delta S_1/2$). The sequence effect on fatigue life (a) becomes more pronounced as ΔS_2 becomes smaller. Source: Ref 21

Although residual stresses may be considered equivalent to mechanically imposed mean stresses when the cyclic stress is low, their effect on fatigue is less than that indicated by their initial value when the stress or strain is high, because the residual stress is "washed out" by repeated slip. The nominal maximum stress is defined as the algebraic sum of the alternating stress and the mean stress. When the nominal maximum stress is larger than the yield strength, S_y, there is little influence on the residual stress regardless of its original magnitude, and the behavior in fatigue will be similar to that of a stress-free member under fully reversed loading. Most change in residual stress occurs during the first few cycles.

Discontinuities. Many features of a material that are not reflected by the usual bulk mechanical properties may have a large influence on its fatigue resistance. Porosity and inclusions may have little effect on the fatigue behavior of a material, provided that they are less than a certain critical size and are not located in a highly stressed region. The critical size depends on the fracture toughness of the material, shape of the pore or inclusion, and stress intensity at the inclusion or pore. Pores and inclusions larger than this critical size can significantly reduce fatigue life, possibly causing failure during the first load application. Surface discontinuities such as folds, seams, score marks, cracks, and corrosion pits greatly influence fatigue behavior. The detrimental effect of these surface discontinuities on fatigue behavior can be somewhat reduced by surface treatments such as shot peening and surface rolling. Anisotropy of the microstructure can be detrimental to fatigue life, particularly if the tensile component of applied stress is nearly perpendicular to the long dimension of elongated grains or stringers. Because it is impractical to eliminate all discontinuities completely, the quantitative influence of discontinuities must be determined by fatigue tests involving the materials, manufacturing processes, and shapes of the parts in question.

Comparison of fatigue testing techniques can show large differences in the results of a life prediction. Socie (Ref 21) discusses four techniques:

- Load life
- Stress life
- Strain life
- Crack propagation

and the application of each. He makes the point that load life, while most accurate, is generally restricted to real parts and is difficult to apply to new designs. He points out that different load application methods, as in axial versus rotating bending, often make large differences in results (Fig. 29). Socie also cautions the user about sequence effects (Fig. 30). Load history A (Fig. 30b) and load history B (Fig. 30c) have similar-appearing strain histories with totally different stress-strain response and fatigue life (Fig. 30a).

Ultimately, the fatigue analyst will be required to include and correlate a number of material, shape, processing, and load factors in order to identify the critical locations within a part and to describe the local stress-strain response at those critical locations. The ability to anticipate pertinent factors will greatly affect the final accuracy of the life prediction.

Load data gathering is one remaining topic that must be included in any discussion of fatigue. Reference 21 discusses three load histories, suspension, transmission, and bracket vibration, that typify loads found in the ground vehicle industry. Additionally, there are vastly different histories unique to other industries, like the so-called ground-air-ground cycle in aeronautics. Without the ability to completely and accurately characterize anticipated and, occasionally, unanticipated customer use and resultant loads, the analyst will not be able to predict accurately the suitability of a new or revised design.

The last several years have seen a major change in the ability to gather customer or simulated customer load data. Testing methods have progressed from bulky, multichannel analogue tape recorders (where it took days or weeks before results were available) through portable frequency-modulated telemetry packages (where analysis could be performed immediately at a remote site) to hand-held packages capable of data acquisition and analysis on board the test vehicle in real time. Microelectronics is further reducing size and improving reliability to the point that data can be gathered from within small, complex, moving, hostile assemblies, such as engines.

REFERENCES

1. R.W. Hertzberg, *Deformation and Fracture Mechanics of Engineering Materials*, John Wiley & Sons, 1976
2. D.J. Wulpi, *Understanding How Components Fail*, American Society for Metals, 1985
3. Fatigue and Microstructure, in *Proceedings of the ASM Materials Science Seminar*, American Society for Metals, 1979
4. *Metallic Materials and Elements for Aerospace Vehicle Structures*, MIL-HDBK-5B, *Military Standardization Handbook*, U.S. Department of Defense, 1987
5. *Metallic Materials and Elements for Aerospace Vehicle Structures*, Vol 1, MIL-HDBK-5B, *Military Standardization Handbook*, U.S. Department of Defense, Sept 1971, p 2-29
6. R.C. Juvinall, *Engineering Considerations of Stress, Strain and Strength*, McGraw-Hill, 1967
7. N.E. Dowling, W.R. Brose, and W.K. Wilson, Notched Member Fatigue Life Predictions by the Local Strain Approach, in *Fatigue Under Complex Loading: Analyses and Experiments*, R.M. Wetzel, Ed., Society of Automotive Engineers, 1977
8. J.A. Graham, Ed., *Fatigue Design Handbook*, Society of Automotive Engineers, 1968
9. H.O. Fuchs and R.I. Stephens, *Metal Fatigue in Engineering*, John Wiley & Sons, 1980
10. Special Publication P-109, in *Proceedings of the SAE Fatigue Conference*, Society of Automotive Engineers, 1982
11. R.C. Rice, Ed., *Fatigue Design Handbook*, 2nd ed., Society of Automotive Engineers, 1988
12. J.T. Ransom, *Trans. ASM*, Vol 46, 1954, p 1254-1269
13. "Fatigue Properties," Technical Report, SAE J1099, Society of Automotive Engineers, 1977
14. P.H. Wirsching and J.E. Kempert, A Fresh Look at Fatigue, *Mach. Des.*, Vol 48 (No. 12), 1976, p 120-123
15. L.E. Tucker, S.D. Downing, and L. Camillo, Accuracy of Simplified Fatigue Prediction Methods, in *Fatigue Under Complex Loading: Analyses and Experiments*, R.M. Wetzel, Ed., Society of Automotive Engineers, 1977
16. R.E. Peterson, *Stress Concentration Design Factors*, John Wiley & Sons, 1974
17. R.J. Roark, *Formulas for Stress and Strain*, 4th ed., McGraw-Hill, 1965
18. J.M. Potter, Spectrum Fatigue Life Predictions for Typical Automotive Load Histories and Materials Using the Sequence Accountable Fatigue Analysis, in *Fatigue Under Complex Loading: Analyses and Experiments*, R.M. Wetzel, Ed., Society of Automotive Engineers, 1977
19. D.V. Nelson and H.O. Fuchs, Predictions of Cumulative Fatigue Damage Using Condensed Load Histories, in *Fatigue Under Complex Loading: Analyses and Experiments*, R.M. Wetzel, Ed., Society of Automotive Engineers, 1977
20. S.D. Downing and D.F. Socie, Simple Rainflow Counting Algorithms, *Int. J. Fatigue*, Jan 1981
21. D.F. Socie, "Fatigue Life Estimation Techniques," Technical Report 145, Electro General Corporation